Accepted Manuscript

Depositional environment and hydrocarbon source potential of the Lower Miocene oil shale deposit in the Aleksinac Basin (Serbia)

Achim Bechtel, Klaus Oberauer, Aleksandar Kostić, Reinhard Gratzer, Vladimir Milisavljević, Nikoleta Aleksić, Ksenija Stojanović, Doris Groß, Reinhard F. Sachsenhofer

PII: S0146-6380(17)30382-0
DOI: https://doi.org/10.1016/j.orggeochem.2017.10.009
Reference: OG 3630

To appear in: *Organic Geochemistry*

Received Date: 5 September 2017
Revised Date: 17 October 2017
Accepted Date: 22 October 2017

Please cite this article as: Bechtel, A., Oberauer, K., Kostić, A., Gratzer, R., Milisavljević, V., Aleksić, N., Stojanović, K., Groß, D., Sachsenhofer, R.F., Depositional environment and hydrocarbon source potential of the Lower Miocene oil shale deposit in the Aleksinac Basin (Serbia), *Organic Geochemistry* (2017), doi: https://doi.org/10.1016/j.orggeochem.2017.10.009

This is a PDF file of an unedited manuscript that has been accepted for publication. As a service to our customers we are providing this early version of the manuscript. The manuscript will undergo copyediting, typesetting, and review of the resulting proof before it is published in its final form. Please note that during the production process errors may be discovered which could affect the content, and all legal disclaimers that apply to the journal pertain.

ACCEPTED MANUSCRIPT

Depositional environment and hydrocarbon source potential of the Lower Miocene oil shale deposit in the Aleksinac Basin (Serbia)

Achim Bechtel [a*], Klaus Oberauer [a], Aleksandar Kostić [b], Reinhard Gratzer [a], Vladimir Milisavljević [b], Nikoleta Aleksić [b], Ksenija Stojanović [c], Doris Groß [a], Reinhard F. Sachsenhofer [a]

[a] *Department of Applied Geosciences and Geophysics, Montanuniversitaet Leoben, Peter-Tunner-Str. 5, A-8700 Leoben, Austria*

[b] *Faculty of Mining and Geology, University of Belgrade, Đušina 7, 11000 Belgrade, Serbia*

[c] *Faculty of Chemistry, University of Belgrade, Studentski trg 12-16, 11000 Belgrade, Serbia*

* Corresponding author. Tel.: +43 3842 402 6356.

E-mail address: Achim.Bechtel@unileoben.ac.at (A. Bechtel)

ABSTRACT

The most prolific oil shale deposit in Serbia is located in the Aleksinac Basin and is assigned to the Lower Miocene. Depositional environments and hydrocarbon potential were assessed for the Aleksinac oil shale and coal layers through bulk geochemical, organic petrographical, biomarker, and carbon isotope data from core samples from a single well. Maturity parameters (vitrinite reflectance, T_{max}, biomarker isomerisation ratios) prove that the organic matter (OM) is immature. A lower lacustrine oil shale sequence is comprised of alternating sandstone and clay-rich rocks and some thin coal beds, indicating strong variations in depositional environment. This stratum is covered with thick sandstone (50 m) terminated by

ACCEPTED MANUSCRIPT

ACCEPTED MANUSCRIPT

the main 4 m thick coal seam that was deposited in a low-lying mire, as evidenced by high total sulfur and mineral matrix contents. The plant input was dominated by angiosperms. A relative rise in water level led to the drowning of the swamp and to the deposition of a 60 m thick upper oil shale in a lacustrine environment. The OM of the oil shale is dominated by kerogen Type I (lamalginite). Biomarker data suggest a stratified water column that likely formed due to differences in salinity. The stratified water column led to a strictly anoxic environment and photic zone euxinia in a mesosalinar, hydrologically closed lake, which enabled the accumulation of uncommonly high amounts of organic material (average TOC: 18.0 wt%) with excellent preservation (average HI: 743 mg HC/g TOC).

Keywords: Aleksinac Basin; Biomarkers; Hydrocarbons; Maceral composition; Oil shale; Organic matter maturity; Stable isotopes

1. Introduction

Organic matter (OM) rich sediments, including oil shale and coal, are often deposited in lacustrine, fault-controlled sedimentary basins where they may serve as excellent petroleum source rocks (Carroll and Bohacs, 1999; Sachsenhofer et al., 2003). In Serbia, many lacustrine basins were formed during different tectonic phases between the Oligocene to Pliocene. The basins are associated with local crustal extension or transtension causing high subsidence rates (Marović et al., 2002). A significant number of these basins host oil shale discoveries and deposits (Ercegovac et al., 2003; 2009).

This study focuses on the Aleksinac Basin, located about 200 km southeast of Belgrade (Fig. 1). The Aleksinac Basin is filled by Lower and Upper Miocene sediments. The Lower Miocene succession ("Aleksinac series") includes marginal lacustrine sediments with thick oil shale layers and several thin coal seams (Fig. 2).

ACCEPTED MANUSCRIPT

ACCEPTED MANUSCRIPT

The Aleksinac deposit has been known for more than 120 years because of a long tradition of coal mining, which started in 1893 in opened outcrops. The Aleksinac coal mine was closed in 1990 after a major disaster in 1989 (Simeunović et al., 2003). The first exploration related to oil shale was performed in 1937, near Subotinac village, in an exploration trench on the right bank of the Moravica River (Fig. 3). After several initial testings, technological analyses were done by 1959 in a semi-industrial facility in Pančevo refinery, Serbia (Matić et al., 1959). Test production actually showed that, with applied technology (i.e., ex-situ retorting), expected production from the oil shale with an average oil yield of 10 wt% (Fischer assay) could be about 90 l (80 kg) of oil and 400 m^3 of gas per ton of shale (Ercegovac et al., 2003; 2009). The "Dubrava" block (2.7 km^2 area) was reported to have total oil shale reserves of 353 million tonnes: 232 million tonnes for the upper and 121 million tonnes for the lower oil shale layer (Petrović, 2012).

The aims of this study are to reveal vertical variations in amount and type of OM, to determine the petroleum potential and to reconstruct the depositional environment of oil shale and the main Aleksinac coal seam. Bulk geochemical parameters, as well as the composition of lipids (biomarkers) and stable isotope ratios of TOC and carbonate were determined. The data are discussed together with the results from organic petrography (maceral description and vitrinite reflectance).

2. Geological setting

Numerous tectonic events resulted in the formation of small lacustrine basins in the territory of present-day Serbia, especially between the Oligocene and Pliocene. Those events are related genetically to the formation and evolution of the large Pannonian Basin (Marović et al., 1999; Obradović et al., 2000). The lacustrine sediments in these small Neogene basins alternate with alluvial and swamp deposits that represent different facies zones.

ACCEPTED MANUSCRIPT

The Aleksinac Basin is located south of the Pannonian Basin (Peri Pannonian Realm), where three geotectonic units were formed due to compressional forces occurring during convergence of several oceanic and continental units between the African and European plates (Dinarides, Serbian Macedonian Massif and Carpatho-Balkanides; Fig. 1). All subduction-compressional processes in these terrains were largely completed by the end of the Cretaceous. Individual rift basins were formed at the southern rim of the Pannonian Basin during the Miocene. In Ottnangian to Badenian time, fast subsidence was mostly the result of crustal and lithospheric extension and limited to areas of active normal faulting (syn-rift phase). The syn-rift phase was followed by a Late Miocene to Pliocene post-rift phase (Marović et al., 2002).

The Aleksinac Basin covers the area between the Južna Morava River and its right affluence, the Moravica River (Figs. 1 and 3). The oil shale deposit was discovered between the city of Aleksinac and village of Subotinac in a 1.5–2.5 km wide and 8 km long belt and covers an area of 13.7 km^2.The topography is generally mildly undulating, with hilly areas in the east fringe part of the basin. The elevations in the deposit area range from about 150 to 280 m above sea level.

The north-south trending belt of the deposit is divided into three major blocks, from north to south named: “Dubrava”, “Morava” and “Logorište” (Fig. 3a). The blocks are separated by fault zones, and their western borders correspond to the major tectonic dislocations.

The Aleksinac deposit has a very complex structure, due to a significant post-depositional tectonic activity that caused folding, dip-slip and strike-slip faulting, uplift and erosion. The layers are increasingly compressed from east to west, and are thus bended and dipping steeply, and are cross cut by fault zones of dominantly NE–SW direction. The northern border of the deposit is at the interception of a major fault (Fig. 3a), with an outcrop belt (northernmost part of “Dubrava” block); the east border is represented by the outcropping belt of coal and oil shale, and the south border is only cultural, not geologic (Aleksinac town).

ACCEPTED MANUSCRIPT

According to previous sedimentological analysis, four different facies were distinguished in the Lower Miocene Aleksinac series (Figs. 2 and 3). The basal series is formed by an alluvial facies and is represented by reddish clastic sediments including coarse grained, weakly cemented conglomerate, conglomeratic sandstone and claystone. These sediments rest directly on crystalline schists of Precambrian to Cambrian age. The main part of the marginal-lacustrine facies contains two layers of oil shale with the main Aleksinac coal seam (2–6 m thick) between them (Petković and Novković, 1975; Jelenkovićet al., 2008). While the lower oil shale layer (up to 60 m thick; Petrović, 2012) alternates with siliciclastic rocks like clayey and mica sandstone and some thin coal lenses with thicknesses from 0.2 to 0.8 m, the upper oil shale layer, up to 80 m thick, is generally uniform (Kašanin-Grubin et al., 1997; Novković and Grgurović, 1992). These organic-rich sequences are characterized by thin lamination, preservation of plant leaves and absence of bioturbation (Obradović et al., 1997), which requires permanent stratification of the water body and anoxic conditions. Bituminous marlstone deposited in a deeper lake facies (intrabasinal facies) form the uppermost unit of the Aleksinac series.

After the deposition of the Lower Miocene clastites, strong tectonic deformation occurred in the area, resulted in their folding and faulting, uplifting and partial erosion. During the Upper Miocene, the Aleksinac basin area has been subsided again and covered by coarser clastites (the Red clastic series; Fig. 2).

3. Samples and methods

Eighty-nine samples were collected from the deviated borehole BD-4drilled near the village of Subotinac in the “Dubrava”block, 9 km north of Aleksinac town (Fig. 3). They are composite samples typically representative of a core interval 2 m long, which corresponds roughly to 1.5 m of true thickness. All given depths represent true stratigraphic depth below the well top.

ACCEPTED MANUSCRIPT

Representative composite samples were dried, ground and powdered. The samples were taken within a true thickness interval of 13–213 m and represent different lithologies (bituminous marlstone, oil shale, coal, sandstone, clay; Fig. 3c), but most samples are dark gray to gray shale. There are 44 samples from the upper oil shale sequence (above the main coal seam) and 41 samples from the lower sequence (below the main coal seam). The samples Dub-46 and Dub-47 from the top of the main coal seam represent oil shale with intercalations of coaly material, while samples Dub-48 and Dub-77 are "clean" coal samples. All samples from the upper sequence and about half samples from the lower sequence are from oil shale beds.

3.1. Carbon, total sulfur and Rock-Eval pyrolysis analyses

Total carbon (TC) and total sulfur (S) contents of all samples (89) were determined on pulverised sample material (100–150 mg) using an Eltra Helios C/S Analyser. Total organic carbon (TOC) content was determined with the same instrument on samples pre-treated with 50% phosphoric acid. Total inorganic carbon (TIC) contents were calculated by the difference between TC and TOC. TIC contents were used to calculate calcite equivalent percentages ($calcite_{eq}$ = 8.34 x TIC). These data are used to mirror changes of carbonate contents in the profile, assuming calcite as single carbonate mineral.

Depending on the TOC content, 10–50 mg of each pulverized sample was analysed by Rock-Eval pyrolysis. Based on TOC and Rock Eval data and the position within the well, samples were selected for maceral and biomarker analyses and stable isotope analysis of TOC and carbonate.

3.2. Organic petrography

For organic petrographical investigations, 21 polished blocks of selected oil shale samples and two coal samples from the main coal seam (Dub-48) and the lower sequence

ACCEPTED MANUSCRIPT

(Dub-77) were prepared. Microscopic analysis was performed using a Leica MPV microscope and oil immersion objectives on crushed samples (grain size ≤ 1.5 mm) embedded in epoxy resin. The maceral composition was assessed semi-quantitatively with an incident light Leica MPV microscope using reflected white light and fluorescent light and oil immersion objectives (50× magnification). Around 1000 points per polished block were counted using the single scan method (Taylor et al., 1998).

Vitrinite reflectance was measured using a 100× objective in non-polarized light at a wavelength of 546 nm (Taylor et al., 1998). Results are presented as mean random reflectance values (%Rr).

3.3. Organic geochemistry (biomarker analysis)

For organic geochemical analysis, portions of 28 selected composite samples from the upper oil shale layer, the main coal seam, the lower oil shale layer and from a sandstone interbedded with coal lenses were extracted for approximately 1 h using dichloromethane (DCM) in a Dionex ASE 200 accelerated solvent extractor. Asphaltenes were precipitated from a *n*-hexane-DCM solution (80:1, v:v) and separated by centrifugation. The *n*-hexane-soluble fractions were separated into NSO compounds, saturated and aromatic hydrocarbons using medium pressure liquid chromatography (MPLC) with a Köhnen-Willsch instrument (Radke et al., 1980).

The saturated and aromatic hydrocarbon fractions were analyzed using a gas chromatograph equipped with a 60 m DB-5MS fused silica column (i.d. 0.25 mm; 0.25 mm film thickness) and coupled to a ThermoFisher ISQ quadrupole mass spectrometer (GC–MS system). The oven temperature gradient was programmed from 40 °C to 310 °C at 4 °C/min, followed by an isothermal period of 40 min. Helium was used as carrier gas. The sample was injected splitless, with the injector temperature at 270 °C. The spectrometer was operated in the EI (electron ionization) mode over a scan range from *m*/*z* 50 to 600 (0.7 s total scan). Data

ACCEPTED MANUSCRIPT

were processed using an Xcalibur data system. Individual compounds were identified on the basis of retention time in the total ion current (TIC) chromatogram and by comparison of the mass spectra with published data. Relative percentages and absolute concentrations of different compound groups in the saturated and aromatic hydrocarbon fractions were calculated using peak areas in the TIC chromatograms in relation to those of internal standards (deuterated *n*-tetracosane and 1,1´-binaphthyl, respectively), or by integration of peak areas in appropriate mass chromatograms using response factors to correct for the intensities of the fragment ion used for quantification of the total ion abundance. The concentrations were normalized to the TOC content.

3.4. Stable carbon isotope analysis

For bulk carbon isotope analyses of TOC, 82 powdered samples were treated with HCl to remove inorganic carbon. De-carbonated rock samples were placed into tin foil boats and combusted using an elemental analyser (Flash EA 1112) at 1020 °C in an excess of oxygen. The resulting CO_2, separated by column chromatography, was analysed online by a ThermoFisher DELTA-V isotope ratio mass spectrometer. The $^{13}C/^{12}C$ isotope ratios of the CO_2 were compared with the corresponding ratio in a monitoring gas, calibrated against the Vienna-Pee Dee Belemnite (V-PDB) standard by the NBS-19 reference material. Stable isotope ratios are reported in delta notation ($\delta^{13}C$, Coplen, 2011) relative to the V-PDB standard. The reproducibility of the total analytical procedure is in the range of 0.1–0.2‰.

For the decomposition of carbonates for stable isotope analysis, weighed portions of the samples were evacuated and flooded with He using the Gasbench II (ThermoFisher). Carbon and oxygen isotope measurements were performed by addition of 100% H_3PO_4 to the samples heated at 70 °C using a GC PAL online system and subsequent analysis of ^{13}C and ^{18}O by a ThermoFisher DELTA-V isotope ratio mass spectrometer (ir-MS). The results are reported

ACCEPTED MANUSCRIPT

relative to the Pee Dee Belemnite (PDB) standard for both $\delta^{13}C$ and $\delta^{18}O$. The reproducibility was better than 0.2‰.

4. Results and interpretation

4.1. Bulk geochemical parameters

Calcite equivalent percentages ($calcite_{eq}$) in layers below the main coal seam are typically between 0 and 20 wt% (13.7 wt% on average in the lower oil shale layer) and tend to be lower than in samples overlying it (21.6 wt% on average in the upper oil shale layer) (Fig. 4a). In the main coal seam carbonate contents are around 5 wt% and rise in the lowermost 7 m thick interval of the upper oil shale layer to a maximum of 45 wt% (sample Dub-42). Most samples in the upper oil shale layer show $calcite_{eq}$ percentages between 10 and 30 wt%, without a clear depth trend (Fig. 4a). Samples representing bituminous marlstones show enhanced $calcite_{eq}$ varying between 22 and 44 wt%.

The average TOC content of the samples from the lower oil shale layer (146–176 m) is 19.9 wt%. Highly variable TOC contents in the different beds below the main coal seam are caused by the alternation of oil shale, sandy and coaly clay. The TOC content of the main coal seam is high (up to 63 wt%) and decreases gradually upwards (Fig. 4b). With the exception of the lowermost sample (25.3 wt% TOC), TOC contents in the lower part of the upper oil shale layer (86–52 m) vary around 10 wt%. TOC contents in its upper part (52–26 m) are higher and reach 42 wt% in sample Dub-12 at 38.5 m (Fig. 4b).

Total sulfur contents in most samples vary between 2 and 4 wt% with the highest contents in the lower oil shale layer (up to 11 wt%). Bituminous marlstones are characterized by low sulfur contents (Fig. 4e). The high sulfur contents in coal and their variability (3.7–7.5 wt%; Fig. 4e) are most probably a result of alkaline, calcium-rich surface waters and changing pH values (Casagrande, 1987). Consistent with this interpretation, TOC/S ratios of most oil shale samples (2.7–9.4; Fig. 4f) are in the range reported as typical for “normal marine” to

ACCEPTED MANUSCRIPT

freshwater environments (Berner, 1984). Enhanced TOC contents from 52 m upwards lead to increasing TOC/S ratios (between 5 and 10) indicating sulfate-limitation of pyrite formation.

Below the main coal seam, hydrogen index (HI) values range from 30 to 800 mg HC/g TOC, depending on lithology and OM type. The HI of the clean coal samples fall in the range 116–162 mg HC/g TOC. High HI values of two samples from the main coal seam are caused by the presence of interbedded oil shale intervals (Fig. 4c). A general upward increasing trend of the HI from 500 to values around 900 mg HC/g TOC is observed in the upper oil shale layer (Fig. 4c). T_{max} follows the increasing and decreasing trend of the HI in a range from 412 to 445 °C (Fig. 4d). This indicates that T_{max} values are strongly controlled by kerogen type, as also seen from the low T_{max} obtained from two clean coal samples (414–428°C). The plot of HI against T_{max} is shown in Fig. 5. The diagram illustrates that samples from the lower oil shale layer represent Type I and Type II kerogen (oil prone). Nearly all samples of the upper oil shale layer represent Type I kerogen (highly oil prone). Type III kerogen is present in sandstones, siltstones, clays and coal samples (Fig. 5).

4.2. Organic petrography and vitrinite reflectance

Maceral percentages as well as percentages of mineral matrix and pyrite are listed in Table 1. The vertical variability of maceral group percentages (algal liptinite, terrestrial liptinite, vitrinite, and inertinite) is plotted on a mineral matter free (mmf) basis in Fig. 4g.

Liptinite of algal origin dominates down to 52 m (79–98 vol.% mmf; Fig. 4g). In these layers lamalginite is the most abundant liptinite maceral. Telalginite occurs in minor amounts. Telalginite is derived from large colonial or thick-walled unicellular algae, typified by genera such as *Botryococcus*, found in fresh- and brackish water lakes. Lamalginite includes thin-walled colonial or unicellular algae (Dyni, 2006). While telalginite is typically characterized by a greenish fluorescence colour (Fig. 6a), lamalginite displays yellow to orange colours under fluorescent light (Fig. 6b and d). Below 38.5 m depth, the input of terrigenous OM

ACCEPTED MANUSCRIPT

rises, and increases significantly below 52 m depth. Sporinite as the predominant land plant-derived terrigenous liptinite maceral (Fig. 6b) with cutinite (Fig. 6d) and vitrinite, typically as small particles, also appearing in higher abundances. Inertinite is largely absent in all layers (< 1.2 vol.% mmf). For comparison, two samples from the lower oil shale layer (under the main coal seam) were analysed. Again, lamalginite dominates in both samples (60 and 75 vol.%; Table 1; Fig. 4g). As petrographic results of all studied oil shale samples show, the Aleksinac oil shale is a typical lamosite. Terrigenous OM constitutes between 25 and 40 vol.% and is represented by sporinite and vitrinite.

Framboidal pyrite (Fig. 6c) is common in all samples, but especially abundant in samples from the lower oil shale layer and from the coal seams. Mean diameters of the framboids in the samples vary from 2.3 to 3.7 μm with standard deviations in the range of 1.9 to 3.5 μm. According to the diagram of Wilkin et al. (1996), the data imply formation of the pyrite framboids in the water column (euxinic conditions).

Vitrinite is the major maceral group in the coal samples (~84 vol.% mmf, Table 1; Fig. 4g), both from the main coal seam (Dub-48) and from the lower sequence (Dub-77). Densinite is the prevailing vitrinite maceral, whereas ulminite and gelinite are rare. The vitrinite particles are much bigger than in the oil shale layers. Algal liptinite in form of lamalginite and telalginite is absent in the main coal seam, whereas terrigenous liptinite represented by sporinite, cutinite and fluorinite (Fig. 6e and f) occur in amounts of ~15 vol.% mmf. Inertinite (e.g., funginite) is present in low amounts (0.7 vol.% mmf; Fig. 4g). High percentages of mineral matrix indicate coal formation in a low-lying mire.

In the coal sample from the lower sequence (Dub-77) an average vitrinite reflectance of 0.44 $\%R_r$ (average standard deviation: 0.023) was obtained.

4.3. Organic geochemistry

ACCEPTED MANUSCRIPT

In the past few decades, the analysis of the OM by gas chromatography and mass spectrometry has become important in the reconstruction of depositional environments, as well as for the quantification of the hydrocarbon potential of oil shale and coal (Bechtel et al., 2012; Strobl et al., 2014a, b). Biomarker molecules are used for evaluating the source organisms and for maturity assessment. If the results are accompanied by stable isotope analyses of organic carbon and carbonate, such data can be used to reconstruct changes in carbon cycling during OM deposition (Bechtel and Püttmann, 1997; Sachsenhofer et al., 2003; Bechtel et al., 2008).

The extractable organic matter (EOM) yields vary between 3 and 69 mg/g TOC (average 29 mg/g TOC; Table 2). The extracts from most samples are dominated by NSO compounds (41–80% of EOM) and asphaltenes (6–47% of EOM). The proportion of hydrocarbons is low. Saturated hydrocarbons are predominant over aromatic hydrocarbons and the relative percentages of both together vary between 7 and 33% of the EOM, as typical for sediments and coals of low maturity (Tissot and Welte, 1984).

4.3.1. n-Alkanes and acyclic isoprenoids

The *n*-alkane patterns of the Aleksinac samples are dominated by alkanes of intermediate chain lengths (n-C_{21}–n-C_{25}) and long-chain *n*-alkanes (>n-C_{27}; Fig. 7) with a marked odd over even predominance (CPI between 2.6 and 10.3; Table 2; carbon preference index, according to Bray and Evans, 1961). High relative proportions of long-chain *n*-alkanes (Table 2) are typical for higher terrestrial plants (Eglinton and Hamilton, 1967). The short-chain *n*-alkanes (< C_{20}), which are predominantly found in algae and microorganisms (Cranwell, 1977), are detected in low amounts (< 20% of the total *n*-alkane concentrations). Predominant proportions of short-chain *n*-alkanes (34%) are obtained only from oil shale sample Dub-42 (Table 2). The *n*-alkanes of intermediate molecular weight (n-C_{21}–n-C_{25}), which are reported to originate from aquatic macrophytes (Ficken et al., 2000), photosynthetic bacteria, that

ACCEPTED MANUSCRIPT

synthesise *n*-alkanes ranging from *n*-C_{14} to *n*-C_{23} and non-photosynthetic bacteria that are the sources of C_{20} to C_{27} *n*-alkanes (Neto et al., 1998), are found in relative proportions between 17 and 48% (Table 2). Generally lower relative proportions are found in the extracts from the coal, and highest relative percentages were obtained from the bituminous marlstones.

The distributions of *n*-alkanes with a marked odd over even predominance and maxima at *n*-C_{27} were considered as a reliable proof that the OM originates from higher terrestrial plants (Tissot and Welte, 1984). However, certain non-marine algae (e.g., *Botryococcus braunii*) may contribute to the C_{27}–C_{31} *n*-alkanes (Metzger et al., 1989). The A race of *Botryococcus* is known to biosynthesise exclusively odd carbon numbered *n*-alkadienes and trienes in the C_{25}–C_{31} carbon number range (Metzger et al., 1989), being the precursors for odd-numbered *n*-alkanes (CPI up to 4.7 in immature sediments; Derenne et al., 1997).

The isoprenoids pristane (Pr) and phytane (Ph) are present in considerable abundance in all of the samples (Fig. 7). The Pr/Ph values are low (< 0.7; Table 2) in the oil shale samples and composite samples containing oil shale with coal intercalations (Dub-46, Dub-47). Most samples from the upper oil shale layer show Pr/Ph ratios between 0.12 and 0.42 (Fig. 8a). Coal samples Dub-77 (lower section) and Dub-48 (main coal seam) are characterized by higher Pr/Ph ratios of 0.96 and 1.57, respectively (Table 2; Fig. 8a).

An influence of different rank on Pr/Ph in the present study can be ruled out. Based on independent molecular parameters (presence of β-carotane and gammacerane; see below), the low Pr/Ph values are consistent with anoxic bottom water conditions during oil shale deposition. Enhanced Pr/Ph ratios in samples containing coaly material imply slightly higher oxygen availability and an effect of increasing contributions of land plants on Pr/Ph values.

4.3.2. Steroids

Steranes are abundant in all oil shale samples (Table 3). The 5α,14α,17α(H) steranes (20R), dominating the 5β,14α,17α(H) isomers, are present in the C_{27}–C_{29} range (Fig. 7,

ACCEPTED MANUSCRIPT

insert), consistent with the low maturity of the samples. The 5α,14α,17α(H) C_{29} sterane (20S) and the 5α,14β,17β(H) C_{29} sterane (20R) also are present in low amounts. In the bituminous marlstones and the oil shales, C_{29} steranes predominate (ca. 50%), followed without distinct trend by C_{28} or C_{27} steranes (Fig. 7, insert). The C_{27}–C_{29} diaster-13(17)-enes are found in the oil shale samples in low contents, using typical mass fragmentogram (*m*/*z* = 257). The C_{27} and C_{29} diasterenes occur in comparable relative abundances, whereas C_{28} diasterenes are less abundant. Steranes could not be quantified in the coal sample Dub-48 due to their very low abundances and only C_{29} diasterenes were detected. Concentrations of steroids (steranes plus diasterenes) vary in the bituminous marlstones sequence from 104 to 583 μg/g TOC, and in the upper oil shale layer between 33 and 401 μg/g TOC (Table 3). In the main coal seam, steroid concentration is only 3 μg/g TOC and in oil shale samples below the main coal seam concentrations vary from 85 to 95 μg/g TOC. No depth trend of steroid concentrations exists within the profile (Fig. 8b).

While algae are the biological source of C_{27} sterols, the predominant primary producers of C_{29} sterols are photosynthetic organisms, including land plants (Volkman, 1986). Freshwater microalgae like ulvophytes and early diverging prasinophyte also produce high abundances of C_{29} sterols. Other plausible candidates include the glaucocystophytes and early divergent red algae (Kodner et al., 2008). The C_{29} steranes in the oil shale samples mainly originate from algae rather than from vascular plants, as petrographic analyses revealed the predominance of macerals of the alginite group. The single occurrence of C_{29} diaster-13(17)-enes in the coal sample is consistent with the predominance of terrigenous OM. Increasing concentrations of C_{29} diaster-13(17)-enes in Middle Jurassic clays of Poland have been reported as indications for an increased terrestrial input (Marynowski et al., 2007).

4.3.3. Hopanoids and related compounds

ACCEPTED MANUSCRIPT

Hopanoids are important constituents of the non-aromatic cyclic triterpenoids of the coal and oil shale samples (Table 3; Fig. 8b). The hopanoid patterns are characterized by 17β,21β-, 17α,21β- and 17β,21α-type hopanes from C_{27} to C_{31}, with C_{28} absent (Fig. 9). The predominant hopanoid in samples of the upper oil shale layer above 55 m is the C_{30} hop-17(21)-ene. Below this depth 17α,21β C_{30} hopane dominates till the main coal seam, where the neohop-13(18)-ene series predominates (Fig. 9). In sample Dub-48 (main coal seam), C_{27} to C_{30} neohop-13(18)-enes are present. Below the coal seam, only the C_{30} neohop-13(18)-ene occurs in high intensities. Beside a series of C_{32} to C_{34} benzohopanes cyclised at C-20 (Hussler et al., 1984), a second series of benzohopanes from C_{31} to C_{33} cyclised at C-16 (Schaeffer et al., 1995) was identified in the aromatic hydrocarbon fractions of most samples (Fig. 10).

The most probable biological precursors of the hopane derivatives found in the samples are bacteriohopanepolyols (Ourisson et al., 1979). These compounds have been identified in bacteria, as well as in some cryptogames (e.g., moss, ferns).

The vertical variation of steroids and hopanoids concentrations is plotted in Fig. 8b, showing their parallel depth trends. Except for the uppermost two samples in the bituminous marlstone sequence, the steroids/hopanoids ratios are below 1.0, suggesting a high contribution of microbial biomass to the OM of the oil shales or partial decay of OM by bacteria during deposition and early diagenesis (Fig. 8c).

Gammacerane is present with moderate concentrations in all layers except in the main coal seam. The gammacerane index (GI) was calculated as the ratio of gammacerane to αβ-C_{30} hopane and varies in the upper oil shale layer between 0.07 and 0.40 (Fig. 8g). Gammacerane is a marker for a stratified water column during source rock deposition, commonly associated with elevated salinity, as in alkaline lakes and lagoonal carbonate evaporites (Sinninghe Damsté et al., 1995). As in the present case, high gammacerane index

ACCEPTED MANUSCRIPT

values (Fig. 8g) are often associated with low Pr/Ph (Fig. 8a) and the presence of carotenoid-derived components (Fig. 8h; Peters et al., 2005).

4.3.4. Diterpenoids, angiosperm-derived triterpenoids

Diterpenoids of the abietane, pimarane, and phyllocladane structural types occur in all samples at variable abundances (2–150 µg/g TOC; Table 3; Fig. 8d). The 16α(H)-phyllocladane predominates by far (Fig. 7). The corresponding aromatic diterpenoids occur in the gas chromatograms of the aromatic hydrocarbon fractions (Fig. 10) and consist of compounds of the abietane type (e.g., abietatetraene, norabietatriene, simonellite and retene). Diterpenoids are important markers for the contribution of gymnosperms (Otto and Wilde, 2001). From the diterpenoids present in the Aleksinac samples, a predominant role of species of the Coniferales families Cupressaceae/Taxodiaceae is implied (Otto and Wilde, 2001; Stefanova et al., 2002).

Non-hopanoid triterpenoids are found in concentrations between 6 and 171 mg/g TOC (Table 3). Saturated and mono-unsaturated compounds consist of des-A-oleanenes, des-A-urs-12-ene, des-A-lupane, olean-12-ene, and olean-13(18)-ene (Fig. 7). Aromatic non-hopanoid triterpenoids include mainly trimethyl-tetrahydrochrysenes and dimethyl-tetrahydropicene (Fig. 10), and minor tetramethyl-octahydropicenes. Non-hopanoid triterpenoids containing the structures typical of the oleanane skeleton, the ursane skeleton, or the lupane skeleton are known as biomarkers for angiosperms (Karrer et al., 1977; Sukh Dev, 1989). These compounds are significant constituents of leaf waxes, wood, roots, and bark (Karrer et al., 1977).

In Fig. 8d the depth trends of concentrations of diterpenoids (average 22 µg/g TOC) and angiosperm-derived triterpenoids (average 63 µg/g TOC) are indicated. The ratio of diterpenoid to the sum of diterpenoid plus angiosperm-derived triterpenoid hydrocarbons (di-/(di + tri)-terpenoids) is applied as a semi-quantitative proxy for the relative contributions of

ACCEPTED MANUSCRIPT

gymnosperms vs angiosperms to the biomass (Bechtel et al., 2008). The data indicate the predominance of angiosperms in most samples (Fig. 8f; Table 3).

4.3.5. Fernenes, arborenes

Fernenes (C_{27}–C_{29}) with Δ^7, Δ^8, and $\Delta^{9(11)}$ double bonds were identified in low amounts (3–20 µg/g TOC) in the saturated hydrocarbon fraction of samples containing coaly material (Dub-45 to Dub-48, Dub-77; Table 3, Fig. 7). Fernenes are found in ferns and some bacteria (e.g., Howard et al., 1984) and have been considered as indicators for floral input, specific to pteridosperms (seed ferns) and coniferophytes (Paull et al., 1998), although their occurrence in an Antarctic lake indicates that bacterial sources must also be considered (Volkman et al., 1986). The presence of onocerane in the coal sample from the main coal seam (Dub-48) supports the presence of ferns or fern-like plants in the peat-forming vegetation (Pearson and Obaje, 1999).

Aromatic triterpenoids with fernane or arborane skeleton were found in all samples in variable concentrations (3–149 µg/g TOC; Table 3). The distinction between aromatized derivatives of fernene and arborene is not possible by GC–MS. The ring-A degraded compounds des-A-arbora(ferna)-tetraene and des-A-arbora(ferna)-triene are present in highest intensities (Fig. 10). Based on the fact that fernenes are only present in coaly samples and that no relationship can be seen between the concentrations of aromatic arborane(fernane)-derivatives and fernenes contents, the aromatic compounds are most probably related to the arborane-type (Fig. 8i). However, the presence of aromatic fernenes cannot be excluded.

The origin of triterpenoids related to the arborane skeleton remains controversial with respect to their possible biological precursors (Hauke et al., 1992, 1995). Arborane derivatives are derived from isoarborinol or arborinone during early diagenesis (Jaffé and Hausmann, 1994). Isoarborinol is present in various families of higher plants (Ohmoto et al., 1970; Hemmers et al., 1989), but geochemical and biosynthetic features have led to the proposal that

ACCEPTED MANUSCRIPT

fossilized isoarborinol (and other sedimentary arborane derivatives) might originate from as yet unknown bacteria (Hauke et al., 1992; Jaffé and Hausmann, 1994).

4.3.6. Carotenoids

In the Aleksinac sediments, β-carotane occurs in the saturated hydrocarbon fractions. The concentrations of β-carotane vary in a wide range between 4 and 295 μg/g TOC in the oil shale layers and are absent in coal samples. In the aromatic hydrocarbons, carotenoids occur in the oil shales predominantly in form of a C_{40} monoaromatic carotenoid (Koopmans et al., 1997; Fig. 10) in concentrations between 1 and 83 μg/g TOC. Again, this carotenoid was not detected in coal samples. The down-hole variation of the sum of total carotenoids concentrations are shown in Fig. 8h.

Carotenoids comprise a wide range of C_{40} compounds produced mainly by photosynthetic organisms (algae). Because carotenoids are easily oxidized, they are rarely found in sediments (Repeta and Gagosian, 1987; Repeta, 1989). However, under highly reducing conditions, the carotenoid skeleton has been reported to be preserved in sedimentary rocks of Permian age (Kluska et al., 2013). The presence of relatively high concentrations of β-carotane, suggests source input dominated by species of halophilic bacteria (Jiang and Fowler, 1986) or cyanobacteria (Brocks et al., 2005).

The aromatic hydrocarbon composition of samples from the upper oil shale is further characterised by the occurrence of C_{14}–C_{21} aryl isoprenoids with a 2,3,6-trimethyl substitution pattern for the aromatic ring and a tail-to-tail isoprenoid chain. These compounds are present in variable abundances, with the C_{19} aryl isoprenoid in greatest abundance (Table 3). Highest concentrations are found in the oil shale interval overlying the main coal seam. In the bituminous marlstone and the uppermost samples of the upper oil shale layer, these compounds are present in very low concentrations insufficient for peak integration (Table 3). The same is true for the samples of the main coal seam and the lower oil shale layer.

ACCEPTED MANUSCRIPT

The identified aryl isoprenoids are derived from carotenoids specific to photosynthetic green sulfur bacteria (*Chlorobiaceae*), as indicated by the occurrence of β-isorenieratane in the oil shale samples Dub-38, Dub-40, and Dub-42 (Summons and Powell, 1987; Brocks and Schaeffer, 2008). In sample Dub-42, β-renierapurpurane is also present, which has been recorded as a potential marker for purple sulfur bacteria (Brocks and Schaeffer, 2008). The data imply that photic zone euxinia was established in the lake after drowning of the mire.

4.4. Stable isotope analyses

Carbon stable isotopes are used to characterize OM in source rocks, and to reconstruct changes in the depositional environment. Fig. 11 shows the vertical variation of $\delta^{13}C$ of total OM. Samples from coaly beds and the main coal seam have typically enriched $\delta^{13}C$ values (–28 to –26‰) than samples taken from the bituminous marlstones and oil shales (–31 to –29‰). This difference can be interpreted as reflecting the ^{13}C-enriched isotopic composition of terrigenous OM and ^{13}C-depleted isotopic composition of phytoplankton. The coal samples Dub-48, Dub-47 and Dub-46 show ^{13}C enrichment due to terrigenous OM input and oxic environment (Fig. 11c). The results are in agreement with published $\delta^{13}C$ values of aquatic OM in lake sediments and with data representing major sources of plant OM (Meyers, 1994).

Interestingly, a negative relationship exists between HI and $\delta^{13}C$ ($R^2 = 0.57$) indicating that a high HI is associated with depleted $\delta^{13}C$ values. As HI reflects OM type, the relationship could simply be explained by variable contributions of land plants. However, a high HI is also indicative for excellent OM preservation under anoxic conditions associated with the activity of anaerobic archaea and bacteria (Vetö et al., 1994). In such environments, accumulation of dissolved CO_2 in the water column, originating from degradation of OM (e.g., sulfate reduction, methane oxidation), is possible. This process is known as "CO_2 recycling" of degradation products. Subsequent incorporation of this CO_2 into the biomass by photosynthetic organisms results in isotopically depleted $\delta^{13}C$ values of the OM preserved in

ACCEPTED MANUSCRIPT

the sediments (Lewan, 1986; Fogel et al., 1988; Frimmel et al, 2004). The fact that samples with high contents of hopanoids are characterized by more negative $\delta^{13}C$ values provides evidence that CO_2 recycling may be involved.

In the upper and lower oil shale, calcite predominates by far over dolomite (< 10% relative contribution to total carbonate). The $\delta^{13}C$ values of total carbonate range from 0.0 to 10.2‰ (Fig. 11d). Generally, less positive values were obtained from the lower oil shale layer. $\delta^{18}O$ ranges from 1.0 to 12.1‰ and shows parallel depth-related trends to $\delta^{13}C$ within the profile (Fig. 11d). Values around 0 are obtained in the bituminous marlstone, where dolomite is present in considerable amounts. Positive $\delta^{13}C$ values are usually interpreted to reflect carbonate precipitated within a brackish/marine environment and indicate a high ratio of evaporation vs precipitation (Anderson and Arthur, 1983), whereas, the obtained $\delta^{18}O$ values fall within the range reported from freshwater carbonate.

In the samples from the upper oil shale layer, a positive relationship ($R^2 = 0.74$) exists between $\delta^{13}C$ and $\delta^{18}O$ values of carbonate, whereas no such relationship exists in samples from the lower oil shale layer (Fig. 12). The relationship between carbon and oxygen isotopic composition is an argument for a long residence time of the water body during deposition of upper oil shale (closed system according to Talbot, 1990). In a restricted (closed) basin, high evaporation/precipitation ratios result in elevated $\delta^{13}C$ and $\delta^{18}O$ values. The lack of covariance between carbon and oxygen isotope ratios in the lower oil shale succession (Fig. 12) suggests a relatively low residence time of the water in the lake (open system according to Talbot, 1990). Such an environment is characteristic of a less restricted basin subjected to periods of increased freshwater inflow.

However, the high $\delta^{13}C$ values found in the sediments of Aleksinac series are unusual for a lacustrine deposit (Anderson and Arthur, 1983), even by taking into account alkaline waters of enhanced salinity. High bioproductivity in the photic zone of the water column may

ACCEPTED MANUSCRIPT

contribute to the shift towards enriched $\delta^{13}C$ values of carbonate (McKenzie, 1985; Hollander and McKenzie, 1991).

5. Discussion

5.1. Maturity

Average vitrinite reflectance of coal and oil shale layers (0.44 $\%R_r$) indicate that the OM is thermally immature. This interpretation is supported by low production index values (PI: ~ 0.01) and the predominance of polar compounds in the EOM. T_{max} of Type I kerogen is a poor maturity parameter, but low T_{max} values of samples with predominant Type III kerogen (410–430 °C) are additional proof for the low maturity of the studied succession. The ratio of S/(S+R)-isomers of C_{31} αβ-hopanes varies between 0.17 and 0.26, distinct from the equilibrium value (0.60, corresponding to early catagenetic stage; Peters et al., 2005), also confirming immature OM. The presence of ββ-hopanes, hopenes and fernenes in the EOM also is a good indication of immature OM. Based on the biomarker composition (e.g., hopanoids) in coal, an even lower thermal maturity of OM is suggested, contrasting the results of vitrinite reflectance measurement. Low, but long-term, temperature influence may have led to increased vitrinite reflectance values of ca. 0.44 $\%R_r$, with only minor changes to the composition of unstable biomarkers and biomolecules (Rybicki et al., 2016). However, in the present case differences in OM-type (i.e., Type I and Type III kerogen) and environmental conditions (e.g., pH, Eh) may result in differences in biomarker composition despite the identical thermal history of the samples (ten Haven et al., 1986; Kostić, 2010).

5.2. Depositional environment

Due to limited information about the layers below the main coal seam, the depositional environment of these samples is not discussed in detail. Highly variable TOC and sulfur

ACCEPTED MANUSCRIPT

contents, as well as increased Pr/Ph ratios and the lack of aryl isoprenoids argue for frequent changes in nutrient supply, water column stratification and salinity.

The main coal seam in borehole BD-4 is represented by samples Dub-48 to Dub-46. These samples show a trend from a shaly coal with high TOC and low mineral matter content (Dub-48) to coaly shale (Dub-46). The presence of alginite and moderately high to high mineral matter contents reflects subaquatic deposition in drowning low-lying mire (stage 1; Fig. 13). High percentages of vitrinite in sample Dub-48 and low percentages of inertinite macerals (< 1 vol.%) reflect the input of higher land plants, which according to biomarker analysis was dominated by angiosperms. The occurrence of fernenes in the main coal seam and in the coal from lower section (Dub-77), as well as the presence of onocerane and abundant neohop-13(18)-enes, suggests rapid deposition of fern-derived OM in the mire (Ageta et al., 1968; Pearson and Obaje, 1999; Garel et al., 2014). A $\delta^{13}C$ value of –26‰ reflects the terrestrial input. Pr/Ph ratios indicate an oxygenated environment during deposition of Dub-48, whereas the rising water table caused anoxic conditions during deposition of the upper part of the main coal seam (Dub-47, Dub-46). Sulfur contents are high in all samples (3.7–7.5 wt%). This together with high percentages of framboidal pyrite indicates either a brackish influence or a carbonate-rich environment with relative high pH values (e.g., Diessel, 1992).

The swamp facies was replaced by a lacustrine environment caused by a rise in relative lake level, probably a result of high subsidence rates. TOC contents decrease significantly in the transition zone, but remain in the order of 10–25 wt% in the lowermost part of the upper oil shale (stage 2: 86–69 m; Fig. 13). Very high percentages of alginite and high HI values (638–886 mg HC/g TOC) indicate the predominance of aquatic OM. Based on the terpenoid hydrocarbons composition angiosperm-dominated vegetation is evidenced, although the relative abundance of gymnosperm-derived biomarkers increases upwards. Increasing water depth allowed the establishment of a stratified water column and photic zone euxinia, as

ACCEPTED MANUSCRIPT

indicated by very low Pr/Ph ratios, the presence of carotenoids derived from β-carotene as well as β-isorenieratane and associated aryl isoprenoids. Upward increasing gammacerane index (GI) values suggest that water column stratification was due to salinity stratification (Sinninghe Damsté et al., 1995). An alkaline lake environment is also supported by high sulfur contents, low TOC/S ratios and locally high carbonate contents. The aquatic OM (mainly algae) is ^{13}C-depleted (–31 to –29‰). Samples with high contents of hopanoids are characterized by lower δ^{13}C values. Therefore, isotopically depleted values are interpreted to reflect enhanced accumulation of dissolved CO_2 within the water column, originating from degradation of OM by bacterial oxidation (Bechtel and Püttmann, 1997; Hertelendi and Vetö, 1991). In these settings dissolved CO_2 in the photic zone may be composed partly of ^{13}C depleted "recycled" CO_2 derived from bacterial decomposition. The relationship between δ^{13}C and δ^{18}O of carbonate (mainly calcite) argues for a long residence time of the water body (closed system according to Talbot, 1990). Positive δ^{13}C values, unusual for freshwater carbonates, can be explained by high evaporation/precipitation ratios and high bioproductivity in the lake water.

An upward decrease in GI during stage 3 (68–51 m; Fig. 13) suggests that water column stratification decreased through time. A parallel decrease in the concentration of carotenoids and a slight increase in Pr/Ph ratios suggest that the weaker water column stratification resulted in a gradual decrease in anoxia. Relative low TOC contents (3–4 wt%) and high percentages of terrestrial macerals (> 60 vol.%) indicate that accumulation of aquatic OM was reduced during the onset of stage 3, which is also reflected by relative low HI values (< 600 mg HC/g TOC). Aquatic bioproductivity recovered thereafter; consequently, TOC contents increased to values around 10 wt% and HI values are in the order of 600–800 mg HC/g TOC.

Oil shale with the highest TOC contents (~20 wt%) were deposited during stage 4 (51–26 m; Fig. 13). A significant increase in TOC/S ratios, despite constantly high sulfur contents, argues for sulfate limitation due to very high OM production and deposition. GI and Pr/Ph

ACCEPTED MANUSCRIPT

ratios imply that salinity stratification and anoxic bottom water conditions persisted during stage 4. Lower concentrations of carotenoids and aryl isoprenoids indicate a diminishing of photic zone anoxia. OM input was dominated by algae and bacteria. Relative high percentages of land plant-derived macerals and reduced HI values indicate that a significant amount of terrestrial OM was deposited during the middle part of stage 4. High concentrations of non-hopanoid triterpenoids in samples Dub-14 and Dub-17 argues for angiosperm-dominated vegetation. OM accumulation decreased during the late stages of oil shale deposition.

The lowermost oil shale sample (Dub-3) within the bituminous marlstone sequence (stage 5; Fig. 13) were deposited in a similar environment as the underlying oil shale. Low sulfur content caused by decreased activity of sulfate-reducers and high TOC/S ratios may reflect a trend towards increased fresh water influx. A lower GI value also supports lower salinity. The primary production of OM is dominated by photosynthetic organisms rather than by bacteria, as evidenced by high alginite percentages, high steroids concentrations, and lower abundances of hopanoids. Diterpenoids predominate over angiosperm-derived triterpenoids, indicating the input of resin-rich terrigenous OM from gymnosperms.

5.3. Petroleum potential

TOC contents and the petroleum potential (S_1 + S_2) are used to characterize the quality of hydrocarbon source rocks (e.g., Peters and Cassa, 1994). Average TOC (18.0 wt%), S_1 + S_2 (115 mg HC/g), and HI values (743 mg HC/g TOC) show the excellent source potential of the upper oil shale layer. Similar average values are recorded for rocks from the lower oil shale layer (TOC: 20.0 wt%; S_1 + S_2: 126 mg HC/g; HI: 620 mg HC/g TOC; Fig. 14). Both oil shale layers include highly oil-prone Type I kerogen. In contrast, samples from sandy and clayey beds underlying the main coal seam are of poor to fair quality. Coal within these layers is characterized by high TOC contents, but relative low generative potential. The amount of hydrocarbons, which can be generated beneath 1 m² of surface area can be calculated using

ACCEPTED MANUSCRIPT

the source potential index (SPI = $[S_1 + S_2] \times h \times \rho/1000$, where h is the thickness of the layer and ρ is bulk density; Demaison and Huizinga, 1994). Adopting a mean oil shale density of 2.078 t/m^3 (Ignjatović et al., 2013), the SPI of the upper oil shale layer (26.5–86 m) and the lower oil shale layer (146–176 m) is 14.2 t HC/m^2 and 7.8 t HC/m^2, respectively.

Few oil yield data from the Aleksinac oil shale are available in publications in English (Čokorilo et al., 2009; Ercegovac et al., 2009). Aside from semi-industrial retort testing in Pančevo refinery (up to 1959), investigations of oil shale quality regarding oil yield (performed in the period 1979–1986) were based on Fischer assay tests (Dyni, 2006). According to more than 2000 analyses (usually on 10 m composite samples), the upper oil shale layer yields on average 8.5 wt% oil, whereas the lower oil shale layer yields on average 11 wt% oil (Ercegovac and Vitorović, 1985, Ercegovac et al., 2003). Newer calculations for the "Dubrava" block (Petrović, 2012) showed that net thickness's average oil yield (Fischer assay) of the upper oil shale layer is 9.9 wt%, and for the lower oil shale layer is 12.5 wt%. Sun et al. (2013) established equations which relate oil yield with TOC content, S_2 and HI for oil shales with different quality. In this study, equations established for oil shales from the Songliao Basin deposited at intermediate water depth are used because of similar kerogen Type (HI ~765 mg HC/g TOC): Oil yield = 0.82×TOC – 0.75; Oil yield = $0.11 \times S_2 - 0.25$. Using the above equations, the average oil yield of the upper oil shale layer based on TOC content and S_2 is 11.8 wt% and 12.2 wt%, respectively. Even higher oil yields (16.4 wt% based on TOC; 14.2 wt% based on S_2) are estimated for the lower oil shale. These data classify the Aleksinac oil shale as high quality according to the Chinese classification.

Considering mining possibilities, it should be mentioned that any valorization, i.e. excavation of oil shale from Aleksinac deposit, should start with the upper oil shale layer at the "Dubrava" block. This block has several important advantages: the most important ones are sufficient reserves for supporting large production rates and favourable setting for implementation of high productive mining technologies. However, there is no relevant

ACCEPTED MANUSCRIPT

documentation on this topic and detailed mining and technological studies are required. According to a reserve report (Petrović, 2012), there is over 230 million tons of oil shale in the upper oil shale layer with average thickness of 54 m, and these can sustain production rate of as much as 5 million tons of oil shale per annum. Anticipating an average oil yield of ~10 wt%, this exploitation rate is equivalent to annual production of some 500×10^3 t of shale oil. Existing initial concepts of oil shale extraction in the Aleksinac deposit assume a start of production with open cast mining, formation of an inner waste dump and subsequent transition to underground mining.

6. Conclusions

Bulk geochemical, micropetrographic and biomarker analysis of the Aleksinac series were carried out in order to determine the depositional environment of the Aleksinac coal and oil shale. In addition, the amount and origin of OM and its petroleum potential was evaluated.

Oil shales in the Aleksinac lacustrine basin are deposited in two thick layers that underlie and overlie the main coal seam. The lower oil shale sequence alternates with siliciclastic rocks and some thin coal beds, indicating strong variations in depositional environment. The lower part of the main coal seam was deposited under oxic conditions and represents a low-lying mire environment. A rising water table caused anoxic conditions during the deposition of the upper part of the coal seam. The peat-forming vegetation was characterized by a predominance of angiosperms over gymnosperms, and ferns.

Increased subsidence rates caused drowning of the Aleksinac coal seam and restoring of a lacustrine environment with the deposition of the 60 m thick upper oil shale layer. An increasing water depth allowed the establishment of a stratified water column due to differences in salinity. This resulted in a strictly anoxic environment and photic zone euxinia in a mesosalinar, hydrologically closed lake and the accumulation of a world-class oil shale deposit. Except for some samples, the OM is dominated by aquatic organisms and bacteria.

ACCEPTED MANUSCRIPT

Depleted $\delta^{13}C$ values of OM result from CO_2 recycling. OM from land plants occurs in minor amounts. Based on abundant algae-derived liptinite macerals and very high HI values, the OM is classified as kerogen Type I. Increased fresh water influx occurred during deposition of bituminous marlstone sequence with thin oil shale intervals. The primary production of OM was dominated by photosynthetic organisms (algae and aquatic plants) rather than by bacteria.

According to T_{max}, biomarker maturation parameters and vitrinite reflectance, the OM of the Aleksinac series is thermally immature. Using the terminology of Peters and Cassa (1994), the lower and upper oil shale layers have a very good to excellent potential to generate oil. The lower oil shale layer shows a source potential index of almost 8 t HC/m^2 and due to the very high thickness, the source potential index of the upper oil shale layer is even higher – over 14 t HC/m^2.

Acknowledgements

The authors thank the Public Company for Underground Coal Exploitation (JPPEU Resavica) for permission to collect samples and providing valuable data. The study was supported by the Ministry of Education, Science and Technological Development of the Republic of Serbia (Projects 176006 and 451-03-01039/2015-09/05). The article benefited from critical remarks by Clifford Walters and an anonymous reviewer.

Associate Editor–**Clifford Walters**

References

1. Ageta, H., Shiojima, K., Arai, Y., 1968. Fern constituents: neohopene, hopene-II, neohopadiene, and fernadiene isolated from *Adiantum* species. Chemical Communications 18, 1105–1107.
2. Anderson, T.F., Arthur, M.A., 1983. Stable isotopes of oxygen and carbon and their application to sedimentologic and palaeoenvironmental problems. In: Arthur, M.A.

ACCEPTED MANUSCRIPT

Anderson, T.F., Kaplan, I.R., Veizer, J., Land, L.S. (Eds.), Stable Isotopes in Sedimentary Geology. Society of Economic Palaeontologists and Mineralogists, Short Course No. 10, pp. I-1 – I-151.

3. Bechtel, A., Püttmann, W., 1997. Palaeoceanography of the early Zechstein Sea during Kupferschiefer deposition in the Lower Rhine Basin (Germany): A reappraisal from stable isotope and organic geochemical investigations. Palaeogeography, Palaeoclimatology, Palaeoecology 136, 331–358.
4. Bechtel, A., Gratzer, R., Sachsenhofer, R.F., Gusterhuber, J., Lücke, A., Püttmann, W., 2008. Biomarker and carbon isotope variation in coal and fossil wood of Central Europe through the Cenozoic. Palaeogeography, Palaeoclimatology, Palaeoecology 262, 166–175.
5. Bechtel, A., Jia, J., Strobl, S.A.I., Sachsenhofer, R.F., Liu, Z., Gratzer, R., Püttmann, W., 2012. Palaeoenvironmental conditions during deposition of the Upper Cretaceous oil shale sequences in the Songliao Basin (NE China): Implications from geochemical analysis. Organic Geochemistry 46, 76–95.
6. Berner, R.A., 1984. Sedimentary pyrite formation: an update. Geochimica et Cosmochimica Acta 48, 605–615.
7. Bray, E.E., Evans, E.D., 1961. Distribution of *n*-paraffins as a clue to recognition of source beds. Geochimica et Cosmochimica Acta 22, 2–15.
8. Brocks, J.J., Schaeffer, P., 2008.Okenane, a biomarker for purple sulfur bacteria (Chromatiacaceae), and other new carotenoid derivatives from the 1640 Ma Barney Creek Formation. Geochimica et Cosmochimica Acta 72, 1396–1414.
9. Brocks, J.J., Love, G.D., Summons, R.E., Knoll, A.H., Logan, G.A., Bowden S.A., 2005. Biomarker evidence for green and purple sulphur bacteria in a stratified Palaeoproterozoic sea. Nature 437, 866–870.

ACCEPTED MANUSCRIPT

ACCEPTED MANUSCRIPT

10. Carroll, A.R., Bohacs, K.M., 1999. Stratigraphic classification of ancient lakes: balancing tectonic and climate controls. Geology 27, 99–102.

11. Casagrande, D.J., 1987. Sulphur in peat and coal. In: Scott, A.C. (Ed.), Coal and Coal-Bearing Strata: Recent Advances. Geological Society Special Publication 32. Geological Society, London, pp. 87–105.

12. Čokorilo, V., Lilić, N., Purga, J., Milisavljević, V., 2009. Oil shale potential in Serbia. Oil Shale 26, 451–462.

13. Coplen, T.B., 2011. Guidelines and recommended terms for expression of stable-isotope-ratio and gas-ratio measurements results. Rapid Communications in Mass Spectrometry 25, 2538–2560.

14. Cranwell, P.A., 1977. Organic geochemistry of Cam Loch (Sutherland) sediments. Chemical Geology 20, 205–221.

15. Demaison, G., Huizinga, B.J., 1994. Genetic classification of petroleum systems using three factors: charge, migration and entrapment. In: Magoon, L.B., Dow, W.G. (Eds.), The Petroleum System – From Source to Trap, American Association Petroleum Geologists Memoir 60, Tulsa, pp. 3–24.

16. Derenne, S., Largeau, C., Hetényi, M., Brukner-Wein, A., Connan, J., Lugardon, B., 1997. Chemical structure of the organic matter in a Pliocene maar-type shale: implicated *Botryococcus* race strains and formation pathways. Geochimica et Cosmochimica Acta 61, 1879–1889.

17. Diessel, C.F.K., 1992. Coal-Bearing Depositional Systems. Springer, Berlin, 721 pp.

18. Dyni, J.R., 2006. Geology and resources of some world oil-shale deposits. USGS Scientific Investigations Report, U.S. Geological Survey, Reston, Virginia, pp. 4–5.

19. Eglinton, G., Hamilton, R.J., 1967. Leaf epicuticular waxes. Science 156, 1322–1335.

ACCEPTED MANUSCRIPT

ACCEPTED MANUSCRIPT

20. Ercegovac, M., Vitorović, D., 1985. Aleksinac oil shale: kerogen, bitumen and evaluation of oil-gas potential. Des Comptes Rendus des Séances de la Société Serbe de Géologie pour l´année 1984, pp. 75–86 (in Serbian, English summary).

21. Ercegovac, M., Grgurović, D., Bajc, S., Vitorović, D., 2003. Oil shales in Serbia: geological and chemical-technological investigations, actual problems of exploration and feasibility studies. In: Vujić, S. (Ed.), Mineral Material Complex of Serbia and Montenegro at the Crossings of Two Millenniums. Margo-Art, Belgrade, pp. 368–378 (in Serbian, English abstract).

22. Ercegovac, M., Vitorović, D., Kostić, A., Životić, D., Jovančićević, B., 2009.Geology and Geochemistry of the "Aleksinac" Oil Shale Deposit (Serbia). Joint 61st ICCP/26th TSOP Meeting, Advances in Organic Petrology and Organic Geochemistry, Gramado, Brazil, p. 13.

23. Espitalié, J., La Porte, J.L., Madec, M., Marquis, F., Leplat, P., Paulet, J., Boutefeu, A., 1977. Methode rapide de characterisation des roches meres de leur potential petrolier et de leur degree dèvolution. Revue de l´insitute Francais du Pétrol 32, 23–42.

24. Espitalié, J., Marquis, F., Barsony, I., 1985. Geochemical logging. In: Voorhess, K.J. (Ed.), Analytical Pyrolysis. Butterworths, Boston, pp. 53–79.

25. Ficken, K.J., Li, B., Swain, D.L., Eglinton, G., 2000. An *n*-alkane proxy for the sedimentary input of submerged/floating freshwater aquatic macrophytes. Organic Geochemistry 31, 745–749.

26. Fogel, M.L., Velinsky, D.J., Cifuentes, L.A., Pennock, J.R., Sharp, J.H., 1988. Biogeochemical processes affecting the stable carbon isotopic composition of particulate carbon in the Delaware Estuary. Carnegie Institute Washington Annual Report Directory 1988, pp. 107–113.

ACCEPTED MANUSCRIPT

ACCEPTED MANUSCRIPT

27. Frimmel, A., Oschmann, W., Schwark, L., 2004. Chemostratigraphy of the Posidonia Shale, SW Germany. I. Influence of sea-level variation on organic facies evolution. Chemical Geology 206, 199–230.

28. Garel, S. Quesnel, F., Jacob, J., Roche, E., Le Milbeau, C., Dupuis, C., Boussafir, M., Baudin, F., Schnyder, J., 2014. High frequency floral changes at the Paleocene–Eocene boundary revealed by comparative biomarker and palynological studies. Organic Geochemistry 77, 43–58.

29. Hauke, V., Graff, R., Wehrung, P., Trendel, J.M., Albrecht, P., Riva, A., Hopfgartner, G., Gülaçar, F.O., Buchs, A., Eakin, P.A., 1992. Novel triterpene-derived hydrocarbons of the arborane/fernane series in sediments: Part II. Geochimica et Cosmochimica Acta 56, 2595–3602.

30. Hauke, V., Trendel, A.J.M., Albrecht, P., Schwark, L., Vliex, M., Hagemann, H., Püttmann, W., 1995. Isoarborinol through geological times: evidence for its presence in the Permian and Triassic. Organic Geochemistry 23, 91–93.

31. Hemmers, H., Guelz, P.G., Marner, F.J., Wray, V., 1989. Pentacyclic triterpenoids in epicuticular waxes from *Euphorbia lathyris* L., *Euphorbiaceae*. Zeitschrift für Naturforschung C 44, 193–201.

32. Hertelendi, E., Vetö, I., 1991. The marine photosynthetic carbon isotopic fractionation remained constant during the Early Oligocene. Paleogeography, Paleoclimatology, Paleoecology 83, 333–339.

33. Hollander, D.J., McKenzie, J.A., 1991. CO_2 control on carbon-isotope fractionation during aqueous photosynthesis: A paleo-pCO_2 barometer. Geology 19, 929–932.

34. Howard, D.L., Simoneit, B.R.T., Chapman, D.J., 1984. Triterpenoids from lipids of *Rhodomicrobium vanniellii*. Archives of Microbiology 137, 200–204.

ACCEPTED MANUSCRIPT

ACCEPTED MANUSCRIPT

35. Hussler, G., Connan, J., Albrecht, P., 1984. Novel families of tetra- and hexacyclic aromatic hopanoids predominant in carbonate rocks and crude oils. Organic Geochemistry 6, 39–49.

36. Ignjatović, M., Rajković, R., Ignjatović, S., Đurđevac Ignjatović, L., Kričak, L., Pantović, R., 2013. Determination of optimal contours of open pit mine during oil shale exploration, by Minex 5.5.3. program. Journal of Process Management – New Technologies 1, 1–9.

37. Jaffé, R., Hausmann, K.B., 1994. Origin and early diagenesis of arborinone/isoarborinol in sediments of a highly productive freshwater lake. Organic Geochemistry 22, 231–235.

38. Jelenković, R., Kostić, A., Životić, D., Ercegovac, M., 2008. Mineral resources of Serbia. Geologica Carpathica 59, 345–361.

39. Jiang, Z., Fowler, M.G. 1986. Carotenoid-derived alkanes in oils from northwestern China. Organic Geochemistry 10, 831–839.

40. Karrer, W., Cherbuliez, E., Eugster, C.H., 1977. Konstitution und Vorkommen der organischen Pflanzenstoffe Ergänzungsband I. Birkhäuser, Basel Stuttgart. 1038 pp.

41. Kašanin-Grubin, M., Glumičić, T., Jovančićević, B., Obradović, J., 1997. Investigation of origin and sedimentation conditions of the Aleksinac oil shales on the basis of inorganic and organic matter composition. Annales Géologiques de la Péninsule Balkanique 61, 325–348 (in Serbian, English summary).

42. Kodner, R.B., Pearson, A., Summons, R.E., Knoll, A.H., 2008. Sterols in red and green algae: quantification, phylogeny, and relevance for the interpretation of geologic steranes. Geobiology 6, 411–420.

43. Koopmans, M.P., de Leeuw, J.W., Sinninghe Damsté, J.S., 1997. Novel cyclised and aromatised diagenetic products of β-carotene in the Green River Shale. Organic Geochemistry 26, 451–466.

ACCEPTED MANUSCRIPT

ACCEPTED MANUSCRIPT

44. Kostić, A., 2010. Thermal evolution of organic matter and petroleum generation modelling in the Pannonian Basin (Serbia). University of Belgrade, Faculty of Mining & Geology, Belgrade, 150 pp. (in Serbian, English summary).

45. Kluska, B., Rospondek, M., Marynowski, L., Schaeffer, P., 2013. The Werra cyclotheme (Upper Permian, Fore-Sudetic Monocline, Poland): Insights into fluctuations of the sedimentary environment from organic geochemical studies. Applied Geochemistry 29, 73–91.

46. Lewan, M.D., 1986. Stable carbon isotopes of amorphous kerogens from Phanerozoic sedimentary rocks. Geochimica et Cosmochimica Acta 50, 1583–1591.

47. Marović, M., Krstić, N., Stanić, S., Cvetković, V., Petrović, M., 1999. The evolution of Neogene sedimentation provinces of central Balkan Peninsula. Bulletin of Geoinstitute Belgrade 36, 25–94 (in Serbian, English summary).

48. Marović, M., Djoković I., Pesić, L., Radovanović, L., Tojić, M., Gerzina, N., 2002. Neotectonics and seismicity of the southern margin of the Pannonian basin in Serbia. EGU Stephan Mueller Special Publication Series, 3, 277–295.

49. Marynowski, L., Zatoń, M., Simoneit, B.R.T., Otto, A., Jędrysek, M.O., Grelowski, C., Kurkiewicz, S., 2007. Compositions, sources and depositional environments of organic matter from the Middle Jurassic clays of Poland. Applied Geochemistry 22, 2456–2485.

50. Matić, D., Lazarević, J., Mijatović. I., 1959. Testing of Aleksinac oil shale in semi-industrial facility in Pančevo town. Chemical Industry 13, 1617–1625 (in Serbian).

51. McKenzie, J.A., 1985. Carbon isotopes and productivity in the lacustrine and marine environment. In: Stumm, W. (Ed.), Chemical Processes in Lakes. John Wiley and Sons, pp. 99–118.

ACCEPTED MANUSCRIPT

ACCEPTED MANUSCRIPT

52. Metzger, P., Villarreal-Rosalles, E., Casadevall, E., Coute, A., 1989. Hydrocarbons, aldehydes and triacylglycerols in some strains of the A race of the green alga *Botryococcus braunii*. Phytochemistry 28, 2349-2353.

53. Meyers, P.A., 1994. Preservation of source identification of sedimentary organic matter during and after deposition. Chemical Geology 144, 289–302.

54. Neto, E.V.D.S., Hayes, J.M., Takaki, T., 1998. Isotopic biogeochemistry of the Neocomian lacustrine and Upper Aptian marine-evaporitic sediments of the Potiguar Basin, Northeastern Brazil. Organic Geochemistry 28, 361–381.

55. Novković, M., Grgurović, D., 1992. A study of actual geological-economic valorisation of some oil shale deposits and findings in Serbia. Documentation of Geozavod, Belgrade (in Serbian).

56. Obradović, J., Djurdjević-Colson, J., Vasić, N., 1997. Phytogenic lacustrine sedimentation – oil shales in Neogene from Serbia, Yugoslavia. Journal of Paleolimnology 18, 351–364.

57. Obradović, J., Vasić, N., Kašanin-Grubin, M., Grubin, N., 2000. Neogene lacustrine sediments and authigenic minerals geochemical characteristics. Annales Géologiques de la Péninsule Balkanique 63, 135–154.

58. Ohmoto, T., Ikuse, M., Natori, S., 1970. Triterpenoids of the Gramineae. Phytochemistry 9, 2137–2148.

59. Otto, A., Wilde, V., 2001. Sesqui-, di-, and triterpenoids as chemosystematic markers in extant conifers–a review. Botanical Review 67, 141–238.

60. Ourisson, G., Albrecht, P., Rohmer, M., 1979. The hopanoids: palaeochemistry and biochemistry of a group of natural products. Pure and Applied Chemistry 51, 709–729.

61. Paull, R., Michaelsen, B.H., McKirdy, D. M., 1998. Fernenes and other triterpenoid hydrocarbons in *Dicroidium*-bearing Triassic mudstones and coals from South Australia. Organic Geochemistry 29, 1331–1343.

ACCEPTED MANUSCRIPT

ACCEPTED MANUSCRIPT

62. Pearson, M.J., Obaje, N.G., 1999. Onocerane and other triterpenoids in Late Cretaceous sediments from the Upper Benue Trough, Nigeria: tectonic and palaeoenvironmental implications. Organic Geochemistry 30, 583–592.

63. Peters, K.E., Cassa, M. R., 1994. Applied source rock geochemistry. In: Magoon, L.B., Dow, W.G. (Eds), The Petroleum System – From Source to Trap, American Association of Petroleum Geologists, Tulsa, OK, pp. 93–117.

64. Peters, K.E., Walters, C.C., Moldowan, J.M., 2005. The Biomarker Guide, Biomarkers and Isotopes in Petroleum Exploration and Earth History, vols. 1 and 2. Cambridge University Press, New York, NY.

65. Petković, K., Novković, M., 1975. Bituminous (oil) shales of Serbia. Geology of Serbia, Caustobioliths VII, 197–210 (in Serbian).

66. Petrović, M., 2012. Reserves report for the Aleksinac oil shale – "Dubrava" block. - JP PEU Resavica, 216 pp. (in Serbian).

67. Radke, M., Willsch, H., Welte, D.H., 1980. Preparative hydrocarbon group type determination by automated medium pressure liquid chromatography. Analytical Chemistry 52, 406–411.

68. Repeta, D.J., 1989. Carotenoid diagenesis in recent marine sediments – II. Degradation of fucoxanthin to loliolide. Geochimica et Cosmochimica Acta 53, 699–707.

69. Repeta, D.J., Gagosian, R.B., 1987. Carotenoid diagenesis in recent marine sediments – I. The Peru continental shelf (15°S, 75°W). Geochimica et Cosmochimica Acta 51, 1001–1009.

70. Rybicki, M., Marynowski, L., Misz-Kennan, M., Simoneit, B.R.T., 2016. Molecular tracers preserved in Lower Jurassic ''Blanowice brown coals" from southern Poland at the onset of coalification: Organic geochemical and petrological characteristics. Organic Geochemistry 102, 77–92.

ACCEPTED MANUSCRIPT

ACCEPTED MANUSCRIPT

71. Sachsenhofer, R.F., Bechtel, A., Reischenbacher, D., Weiss, A., 2003. Evolution of lacustrine systems along the Miocene Mur-Mürz fault system (Eastern Alps, Austria) and implications on source rocks in pull apart basins. Marine and Petroleum Geology 20, 83–110.

72. Schaeffer, P., Adam, P., Trendel, J.-M., Albrecht, P., Connan, J., 1995. A novel series of benzohopanes widespread in sediments. Organic Geochemistry 23, 87–89.

73. Simeunović, V., Gagić, D., Gligorić, Z, Beljić, Č., 2003. The present state and the future of the mineral raw material potential for underground exploitation. In: Vujić, S. (Ed.), Mineral Material Complex of Serbia and Montenegro at the Crossings of Two Millenniums. Margo-Art, Belgrade, pp. 534–550 (in Serbian, English abstract).

74. Sinninghe Damsté, J.S., Kenig, F., Koopmans, M.P., Köster, J., Schouten, S., Hayes, J.M., de Leeuw, J.W., 1995. Evidence for gammacerane as an indicator of water column stratification. Geochimica et Cosmochimica Acta 59, 1895–1900.

75. Stefanova, M., Oros, D.R., Otto, A., Simoneit, B.R.T., 2002. Polar aromatic biomarkers in the Miocene Maritza–East lignite, Bulgaria. Organic Geochemistry 33, 1079–1091.

76. Strobl, S.A.I., Sachsenhofer, R.F., Bechtel, A., Gratzer, R., Gross, D., Bokhari, S.N.H., Liu, R., Liu, Z., Meng, Q., Sun, P., 2014a. Depositional environment of oil shale within the Eocene Jijuntun Formation in the Fushun Basin (NE China). Marine and Petroleum Geology 56, 166–183.

77. Strobl, S.A.I., Sachsenhofer, R.F., Bechtel, A., Meng, Q., 2014b. Palaeoenvironment oft the Eocene coal seam in the Fushun Basin (NE China): Implications from petrography and organic geochemistry. International Journal of Coal Geology 134-135, 24–37.

78. Sukh Dev, 1989. Terpenoids. In: Rowe, J.W. (Ed.), Natural Products of Woody Plants, vol. 1. Springer, Berlin, pp. 691–807.

ACCEPTED MANUSCRIPT

ACCEPTED MANUSCRIPT

79. Sun, P., Liu, Z., Gratzer, R., Xu, Y., Liu, R., Li, B., Meng, Q., Xu, J., 2013. Oil yield and bulk geochemical parameters of oil shales from the Songliao and Huadian basins, China: A grade classification approach. Oil Shale 30, 402–418.

80. Summons R. E., Powell T. G., 1987. Identification of arylisoprenoids in source rocks and crude oils: biological markers for the green sulphur bacteria. Geochimica et Cosmochimica Acta 51, 557–566.

81. Talbot, M. R., 1990. A review of the palaeohydrological interpretation of carbon and oxygen ratios in primary lacustrine carbonates. Chemical Geology 80, 261–279.

82. Taylor, G.H., Teichmüller, M., Davis, A., Diessel, C.F.K., Littke, R., Robert, P., 1998. Organic Petrology. Gebrüder Borntraeger, Berlin, 704 pp.

83. ten Haven, H.L., de Leeuw, J.W., Peakman, T.M., Maxwell, J.R., 1986. Anomalies in steroid and hopanoid maturity indices. Geochimica et Cosmochimica Acta 50, 853–855.

84. Tissot, B.P., Welte, D.H., 1984. Petroleum Formation and Occurrence. 2nd edition, Springer-Verlag, Berlin.

85. Vetö, I., Hetényi, M., Demény, A., Hertelendi, E., 1994. Hydrogen index, as reflecting intensity of sulfidic diagenesis in non-bioturbated, shaly sediments. Organic Geochemistry 22, 299–310.

86. Volkman, J.K., 1986. A review of sterol markers for marine and terrigenous organic matter. Organic Geochemistry 9, 83–99.

87. Volkman, J.K, Allen, D.I., Stevenson, P.I., Burton, H.R., 1986. Bacterial and algal hydrocarbons in sediments from a saline Antartic lake, Ace Lake. Organic Geochemistry 10, 671–681.

88. Wilkin, R.T., Barnes, H.L., Brantley, S.L., 1996. The size distribution of framboidal pyrite in modern sediments: An indicator of redox conditions. Geochimica et Cosmochimica Acta, 60, 3897–3912.

ACCEPTED MANUSCRIPT

ACCEPTED MANUSCRIPT

Fig. 1. Simplified geological map of the Serbian part of the Pannonian Basin with location of the Aleksinac deposit. Inset: (a) position of the study area within the European Alpides, and (b) major tectonic units of the Serbian part of the Pannonian Basin (Marović et al., 2002).

Fig. 2. Stratigraphic column of the Aleksinac Basin (modified after Novković and Grgurović, 1992).

Fig. 3. (a) Aleksinac deposit – overburden thickness map. (b) Geological profile across sampled borehole BD-4. (c) Lithological profile of the borehole with samples position.

Fig. 4. Stratigraphy and depth plot of bulk geochemical parameters; (a) $Calcite_{eq}$: calcite equivalent, (b) TOC: total organic carbon, (c) HI: hydrogen index, (d) T_{max}: temperature of maximum hydrocarbon generation, (e) S: sulfur, (f) TOC/S ratio, and (g) maceral composition on a mineral matter free (mmf) basis.

Fig. 5. Plot of Hydrogen Index (HI) vs T_{max} (according to Espitalié et al, 1985) outlining the kerogen type of different layers in the Aleksinac series.

Fig. 6. Microphotographs of samples from the upper oil shale layer and the main coal seam: (a) Dub-05 under UV light, (b) Dub-40 under UV light, (c) Dub-38 under UV light, (d) Dub-45 under UV light, (e) Dub-48 under white light, (f) Dub-48 under UV light. vit: vitrinite, telalg: telalginite, lamalg: lamalginite, spor: sporinite, cut: cutinite, pyr: pyrite, fluor: fluorinite, res: resinite.

Fig. 7. Total ion chromatograms (TICs) of saturated hydrocarbon fractions of samples from the bituminous marlstone, the upper oil shale, and the Aleksinac coal seam. *n*-Alkanes are labelled according to their carbon number; α-Phyllocladane: 16α(H)- Phyllocladane; ββ-C_{31} Hopane: C_{31} 17β(H)21β(H)-hopane. Insert shows the distribution of steranes (*m/z* 217) in the samples. Std: standard (deuterated tetracosane).

Fig. 8. Distribution of: (a) pristane/phytane (Pr/Ph) ratio, (b) steroid and hopanoid concentrations, (c) steroids/hopanoids ratio, (d) diterpenoid and angiosperm-derived triterpenoid concentrations, (e) sum of diterpenoid and angiosperm- derived triterpenoid concentrations, (f) ratio of diterpenoids to the sum of diterpenoids plus angiosperm-derived triterpenoids, (g) Gammacerane index (GI), (h) carotenoids concentrations, (i) sum of fernenes and of aromatic fernenes (Fern.) or arborenes (Arb.) concentrations.

Fig. 9: Mass chromatograms (*m/z* 191 for hopanoids) of saturated hydrocarbon fractions of samples from the bituminous marlstone, the upper oil shale, and the Aleksinac coal seam.

Fig. 10. Total ion chromatograms (TICs) of aromatic hydrocarbon fractions of samples from the upper oil shale layer. Std: standard (1,1´-binaphthyl).

Fig. 11. Stratigraphy and depth plot: (a) $Calcite_{eq}$: calcite equivalent, (b) TOC: total organic carbon, (c) carbon isotopic composition of TOC, and (d) carbon and oxygen isotopic composition of carbonate (dominated by calcite).

Fig. 12. Cross-plot of carbon vs oxygen isotopic composition of carbonates.

Fig. 13. Cartoon illustrating the depositional environment of the main coal seam and the overlying upper oil shale and bituminous marlstone.

ACCEPTED MANUSCRIPT

ACCEPTED MANUSCRIPT

Fig. 14. Plot of generative potential (S1 + S2) vs total organic carbon (TOC) and resulting oil shale potential according to Peters and Cassa (1994).

Table 1. Data from organic petrographical investigations.

Sample	Depth (m)	Mineral Matrix	Pyrite	Lamalginite	Telalginite	Sporinite	Cutinite	Fluorinite	Vitrinite	Inertinite	Liptinite (alg.)	Liptinite (terr.)	Vitrinite	Inertinite
		(vol%)									(vol% mmf)			
Bituminous marlstone														
Dub-01	13.0	91.3	0.5	6.6		0.2	0.6		0.7	0.0	81.3	9.9	8.8	0.0
Dub-03	23.5	75.6	3.4	17.6	1.6	0.2	0.6		1.0	0.0	91.4	3.8	4.8	0.0
Upper oil shale layer														
Dub-05	28.0	72.2	4.4	20.4	1.0	1.5			0.5	0.0	91.6	6.3	2.1	0.0
Dub-07	31.0	75.4	3.9	17.4	0.9	0.5	0.3		1.6	0.0	88.1	4.2	7.7	0.0
Dub-09	34.0	82.1	3.1	14.4	0.1	0.1			0.1	0.0	98.0	1.0	1.0	0.0
Dub-12	38.5	49.6	5.9	32.8	0.3	7.5	0.7		3.2	0.0	74.4	18.3	7.3	0.0
Dub-14	41.5	62.6	4.8	21.9	0.8	3.8	0.8		5.0	0.4	69.5	14.0	15.2	1.2
Dub-20	50.5	63.8	3.6	25.7	0.4	4.4			2.2	0.0	80.0	13.3	6.7	0.0
Dub-21	52.0	80.2	3.5	13.0		2.2	0.1		1.0	0.0	79.6	14.2	6.2	0.0
Dub-23	55.0	81.1	2.9	10.7	0.2	2.9			2.0	0.2	68.3	18.3	12.5	1.0
Dub-25	58.0	85.0	3.4	4.2		6.0			1.4	0.0	36.2	51.4	12.4	0.0
Dub-27	60.0	83.6	4.0	2.0		7.5			3.0	0.0	16.0	60.0	24.0	0.0
Dub-30	64.5	91.3	2.3	2.3		2.0			2.0	0.0	36.4	31.8	31.8	0.0
Dub-33	69.0	79.3	3.4	13.1	1.6	1.8			0.8	0.0	84.9	10.4	4.7	0.0
Dub-35	72.0	86.8	2.9	4.5	1.3	4.0			0.6	0.0	55.8	38.8	5.4	0.0
Dub-38	76.5	74.3	3.9	20.5		0.4			0.8	0.0	94.3	1.9	3.8	0.0
Dub-40	79.0	87.6	3.2	5.2	0.4	2.8			0.8	0.0	60.6	30.3	9.1	0.0
Dub-42	81.0	82.5	3.7	3.3	0.2	8.9			1.4	0.0	25.7	64.3	10.0	0.0
Dub-45	86.0	67.2	2.5	23.5	1.7	0.8			4.4	0.0	82.9	2.7	14.4	0.0
Main coal seam														
Dub-48	90.5	25.5	3.9			3.3	5.7	1.5	59.6	0.5	0.0	15.2	84.0	0.7
Lower oil shale layer														
Dub-59	152.0	66.0	6.3	15.4	1.1	4.2			7.0	0.0	59.5	15.2	25.3	0.0
Dub-74	174.5	62.8	9.3	20.0	0.8				6.9	0.2	74.6	0.0	24.7	0.7
Coal lense														
Dub-77	194.0	13.8	17.7	0.3	0.6	4.7	4.3		58.0	0.6	1.3	13.1	84.7	0.9

vol%: volume percentages; mmf: mineral matter free basis; Liptinite (alg.): Telalginite + Lamalginite; Liptinite (terr.): Sporinite + Cutinite + Fluorinite

Table 2. Bulk organic geochemical parameters and concentration ratios of *n*-alkanes and acyclic isoprenoids

Sample	**Depth**	**TOC**	**EOM**	**Sat. HC**	**Aro. HC**	**NSO**	**Asphalt.**	**C_{15}–C_{19}/**	**C_{21}–C_{25}/**	**C_{27}–C_{31}/**	**CPI**	**Pr/Ph**

ACCEPTED MANUSCRIPT

	(m)	(wt%)	(mg/g TOC)	(wt%, EOM)				*n*-alkanes	*n*-alkanes	*n*-alkanes		
Bituminous marlstone												
Dub-01	**13.0**	**6.4**	**43.3**	**17**	**4**	**51**	**27**	**0.16**	**0.48**	**0.28**	**3.9**	**0.23**
Dub-02	**17.0**	**6.2**	**23.8**	**26**	**7**	**57**	**9**	**0.08**	**0.40**	**0.43**	**4.1**	**0.20**
Dub-03	**23.5**	**13.1**	**22.2**	**20**	**4**	**56**	**20**	**0.14**	**0.31**	**0.45**	**3.8**	**0.35**
Upper oil shale layer												
Dub-05	**28.0**	**19.8**	**29.7**	**8**	**1**	**44**	**46**	**0.07**	**0.23**	**0.62**	**5.9**	**0.39**
Dub-07	**31.0**	**16.8**	**26.0**	**10**	**2**	**52**	**36**	**0.07**	**0.31**	**0.53**	**4.2**	**0.31**
Dub-09	**34.0**	**11.0**	**25.1**	**19**	**5**	**62**	**13**	**0.09**	**0.42**	**0.40**	**4.4**	**0.20**
Dub-12	**38.5**	**41.9**	**48.4**	**5**	**2**	**61**	**32**	**0.04**	**0.28**	**0.62**	**6.4**	**0.39**
Dub-14	**41.5**	**28.2**	**17.7**	**9**	**4**	**51**	**36**	**0.04**	**0.23**	**0.65**	**5.5**	**0.36**
Dub-17	**46.0**	**28.3**	**21.8**	**15**	**4**	**53**	**28**	**0.03**	**0.24**	**0.68**	**10.3**	**0.37**
Dub-20	**50.5**	**27.3**	**35.6**	**9**	**3**	**42**	**46**	**0.05**	**0.26**	**0.62**	**6.4**	**0.32**
Dub-21	**52.0**	**11.8**	**27.5**	**19**	**3**	**49**	**29**	**0.06**	**0.28**	**0.59**	**5.9**	**0.32**
Dub-23	**55.0**	**11.6**	**36.0**	**16**	**3**	**54**	**26**	**0.13**	**0.24**	**0.54**	**5.3**	**0.48**
Dub-25	**58.0**	**8.8**	**26.8**	**18**	**4**	**68**	**10**	**0.17**	**0.28**	**0.43**	**3.3**	**0.30**
Dub-27	**60.0**	**8.5**	**32.1**	**15**	**3**	**66**	**16**	**0.18**	**0.24**	**0.49**	**3.8**	**0.36**
Dub-30	**64.5**	**3.2**	**68.7**	**22**	**5**	**67**	**7**	**0.15**	**0.54**	**0.21**	**3.4**	**0.12**
Dub-33	**69.0**	**13.4**	**26.2**	**18**	**11**	**41**	**29**	**0.08**	**0.31**	**0.51**	**4.6**	**0.13**
Dub-35	**72.0**	**8.5**	**48.9**	**15**	**4**	**60**	**21**	**0.07**	**0.44**	**0.42**	**4.9**	**0.13**
Dub-38	**76.5**	**19.1**	**26.5**	**15**	**5**	**55**	**24**	**0.06**	**0.33**	**0.53**	**4.8**	**0.13**
Dub-40	**79.0**	**7.0**	**37.7**	**20**	**4**	**69**	**6**	**0.15**	**0.39**	**0.35**	**3.2**	**0.23**
Dub-42	**81.0**	**12.4**	**42.1**	**8**	**3**	**80**	**9**	**0.34**	**0.29**	**0.27**	**2.6**	**0.42**
Dub-45	**86.0**	**25.3**	**11.5**	**10**	**3**	**52**	**35**	**0.10**	**0.27**	**0.53**	**3.8**	**0.59**
Main coal seam												
Dub-46	**87.5**	**32.4**	**19.5**	**9**	**5**	**52**	**34**	**0.15**	**0.22**	**0.49**	**3.0**	**0.45**
Dub-47	**89.0**	**51.6**	**28.8**	**6**	**5**	**56**	**32**	**0.10**	**0.20**	**0.62**	**4.6**	**0.51**
Dub-48	**90.5**	**63.1**	**10.1**	**7**	**7**	**56**	**30**	**0.09**	**0.23**	**0.62**	**5.8**	**1.57**

ACCEPTED MANUSCRIPT

ACCEPTED MANUSCRIPT

Lower oil shale layer												
Dub-59	**152.0**	**27.3**	**26.5**	**9**	**2**	**41**	**47**	**0.09**	**0.29**	**0.53**	**4.5**	**0.49**
Dub-64	**159.5**	**9.3**	**24.1**	**22**	**2**	**51**	**25**	**0.06**	**0.28**	**0.58**	**5.5**	**0.65**
Dub-74	**174.5**	**21.4**	**22.5**	**12**	**5**	**62**	**21**	**0.16**	**0.24**	**0.51**	**4.6**	**0.92**
Coal lense												
Dub-77	**194.0**	**46.5**	**3.9**	**14**	**5**	**59**	**22**	**0.14**	**0.17**	**0.62**	**5.4**	**0.96**

TOC: total organic carbon content; EOM: extractable organic matter yield; Sat.HC: saturated hydrocarbons; Aro.HC: aromatic hydrocarbons; NSO: polar compounds; Asphalt.: asphaltenes; CPI: carbon preference index; Pr/Ph: pristane/phytane ratio.

Table 3: Concentration and concentration ratios of compounds and compound groups in the hydrocarbon fractions.

Sample	**Depth (m)**	**Steroids**	**Hopanoids**	**Diterpenoids**	**Triterpenoids (Angiosperms)**	**Fernenes**	**Fern. or Arb. (Arom.)**	**Carotenoids**	**Aryl isoprenoids**	**GI**	**Di-/(Di + Tri)-terpenoids**
		(µg/g TOC)									
Bituminous marlstone											
Dub-01	**13.0**	**419**	**195**	**150**	**6**	**n.d.**	**7**	**161**	**n.d.**	**0.11**	**0.96**
Dub-02	**17.0**	**583**	**272**	**24**	**18**	**n.d.**	**31**	**130**	**n.d.**	**0.14**	**0.58**
Dub-03	**23.5**	**104**	**213**	**27**	**70**	**n.d.**	**40**	**16**	**n.d.**	**0.28**	**0.28**
Upper oil shale layer											
Dub-05	**28.0**	**55**	**130**	**102**	**22**	**n.d.**	**25**	**23**	**n.d.**	**0.16**	**0.82**
Dub-07	**31.0**	**105**	**243**	**9**	**44**	**n.d.**	**34**	**20**	**n.d.**	**0.18**	**0.17**
Dub-09	**34.0**	**325**	**364**	**15**	**23**	**n.d.**	**15**	**163**	**n.d.**	**0.40**	**0.39**
Dub-12	**38.5**	**36**	**201**	**10**	**50**	**n.d.**	**113**	**12**	**0.8**	**0.19**	**0.16**
Dub-14	**41.5**	**59**	**319**	**4**	**171**	**n.d.**	**149**	**13**	**1.0**	**0.28**	**0.02**
Dub-17	**46.0**	**104**	**537**	**9**	**127**	**n.d.**	**22**	**39**	**1.6**	**0.16**	**0.07**

ACCEPTED MANUSCRIPT

Dub-20	**50.5**	**71**	**177**	**9**	**36**	**n.d.**	**36**	**48**	**1.3**	**0.21**	**0.20**
Dub-21	**52.0**	**79**	**154**	**11**	**18**	**n.d.**	**8**	**35**	**1.3**	**0.12**	**0.38**
Dub-23	**55.0**	**104**	**315**	**18**	**58**	**n.d.**	**15**	**47**	**3.2**	**0.15**	**0.24**
Dub-25	**58.0**	**260**	**566**	**8**	**67**	**n.d.**	**22**	**96**	**2.5**	**0.20**	**0.11**
Dub-27	**60.0**	**125**	**268**	**25**	**48**	**n.d.**	**20**	**72**	**1.2**	**0.32**	**0.35**
Dub-30	**64.5**	**323**	**500**	**22**	**15**	**n.d.**	**3**	**325**	**0.4**	**0.39**	**0.60**
Dub-33	**69.0**	**88**	**169**	**6**	**11**	**n.d.**	**3**	**53**	**0.8**	**0.10**	**0.36**
Dub-35	**72.0**	**401**	**656**	**10**	**30**	**n.d.**	**27**	**281**	**4.9**	**0.28**	**0.26**
Dub-38	**76.5**	**114**	**190**	**8**	**13**	**n.d.**	**6**	**81**	**5.9**	**0.18**	**0.38**
Dub-40	**79.0**	**186**	**447**	**18**	**38**	**n.d.**	**51**	**106**	**8.5**	**0.15**	**0.32**
Dub-42	**81.0**	**63**	**193**	**7**	**64**	**n.d.**	**44**	**110**	**16.6**	**0.12**	**0.09**
Dub-45	**86.0**	**33**	**114**	**3**	**13**	**3.07**	**3**	**6**	**0.4**	**0.07**	**0.16**
Main coal seam											
Dub-46	**87.5**	**63**	**385**	**6**	**129**	**7.47**	**135**	**6**	**n.d.**	**n.d.**	**0.04**
Dub-47	**89.0**	**38**	**130**	**11**	**105**	**14.28**	**135**	**7**	**n.d.**	**n.d.**	**0.10**
Dub-48	**90.5**	**3**	**36**	**17**	**65**	**20.08**	**13**	**0**	**n.d.**	**n.d.**	**0.21**
Lower oil shale layer											
Dub-59	**152.0**	**89**	**274**	**8**	**52**	**n.d.**	**9**	**6**	**n.d.**	**n.d.**	**0.13**
Dub-64	**159.5**	**86**	**402**	**35**	**25**	**n.d.**	**17**	**9**	**n.d.**	**0.09**	**0.59**
Dub-74	**174.5**	**96**	**391**	**9**	**144**	**n.d.**	**57**	**11**	**n.d.**	**0.25**	**0.06**
Coal lense											
Dub-77	**194.0**	**12**	**29**	**2**	**39**	**11.60**	**5**	**0**	**n.d.**	**n.d.**	**0.05**

ACCEPTED MANUSCRIPT

Fern. or Arb. (Arom.): aromatic fernenes or arborenes; GI: gammacerane index; n.d.: not detectable.

ACCEPTED MANUSCRIPT

Figure 01

ACCEPTED MANUSCRIPT

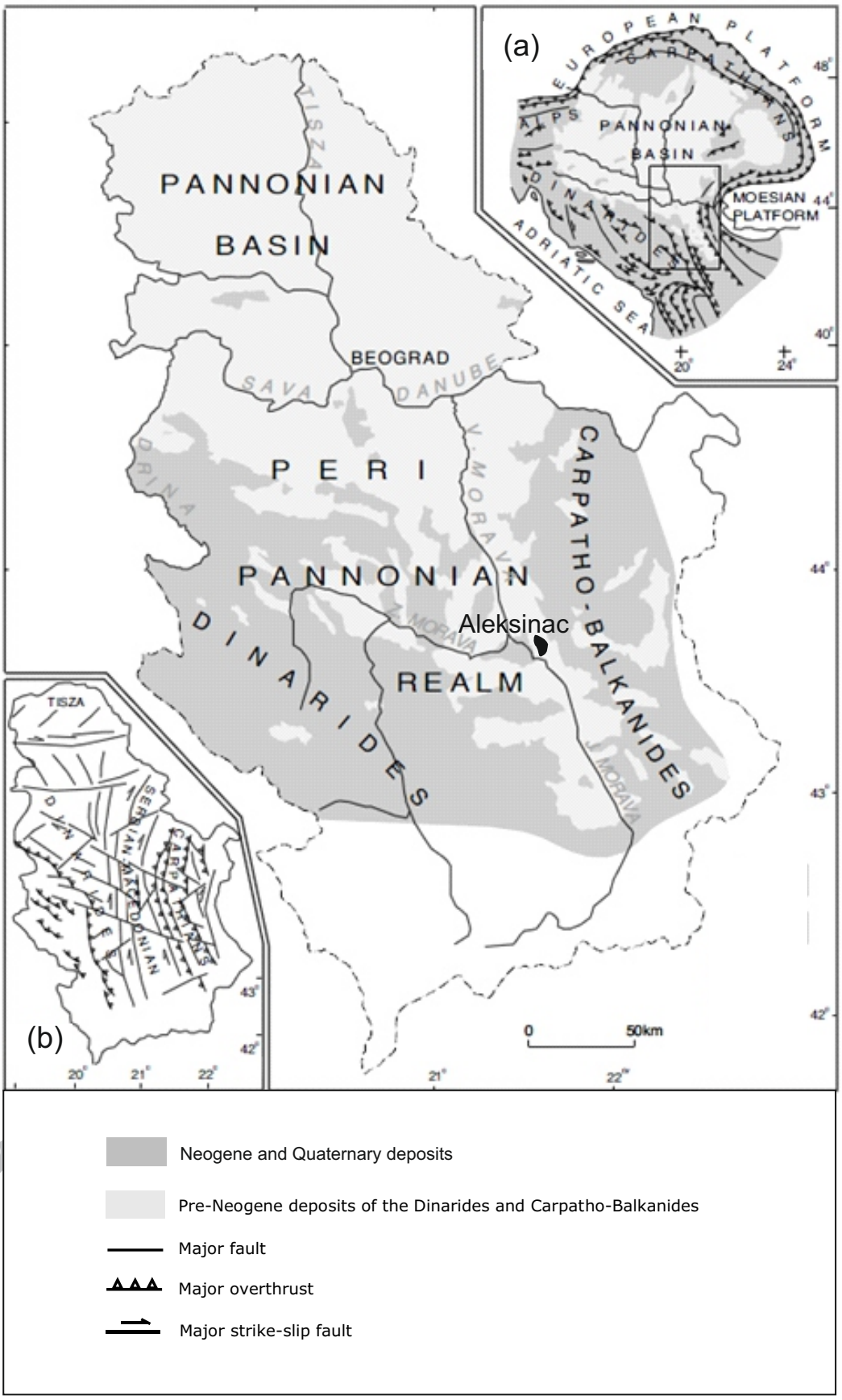

Fig. 1:

Figure 02

ACCEPTED MANUSCRIPT

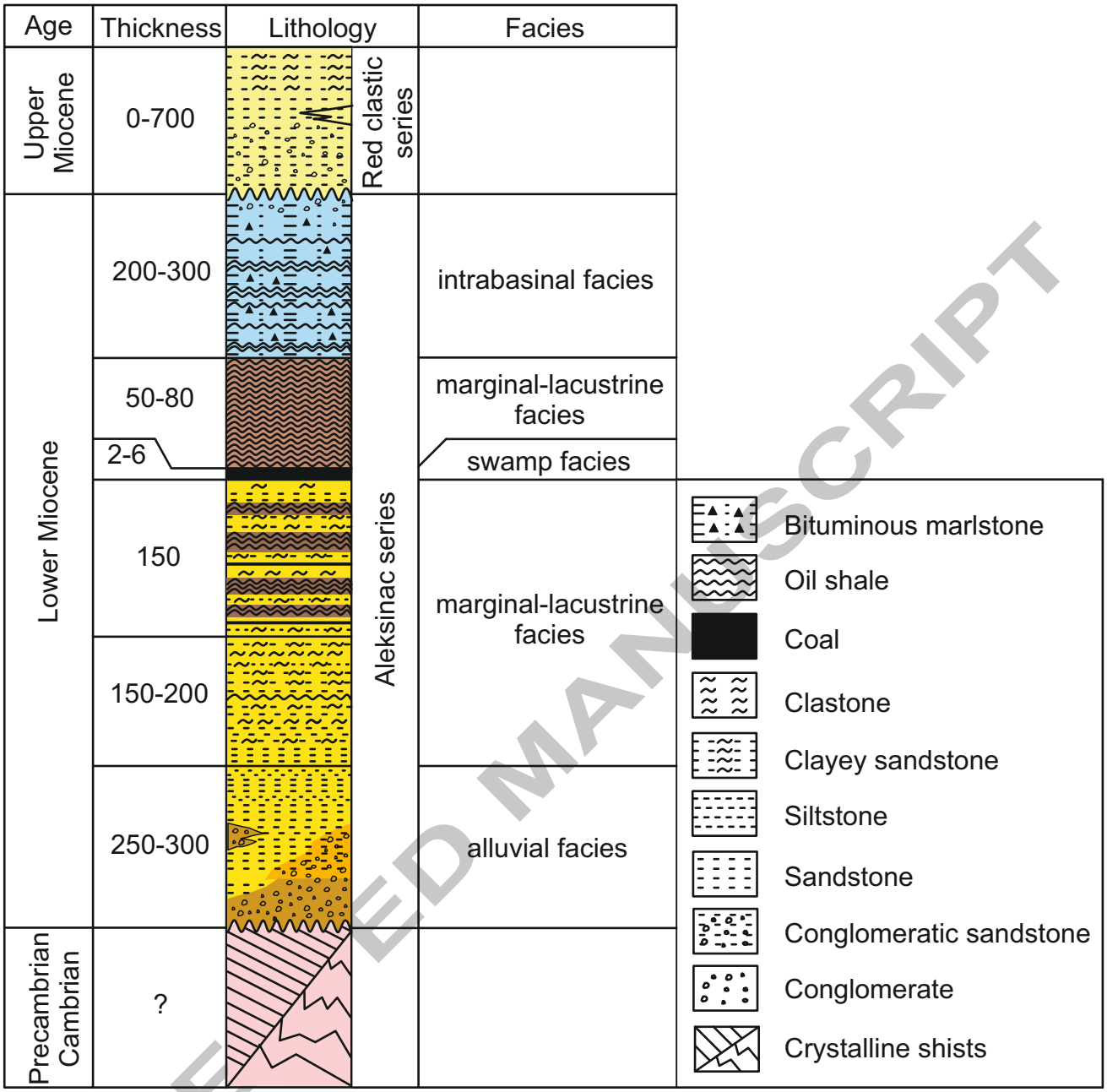

Fig. 2:

ACCEPTED MANUSCRIPT

Figure 02

ACCEPTED MANUSCRIPT

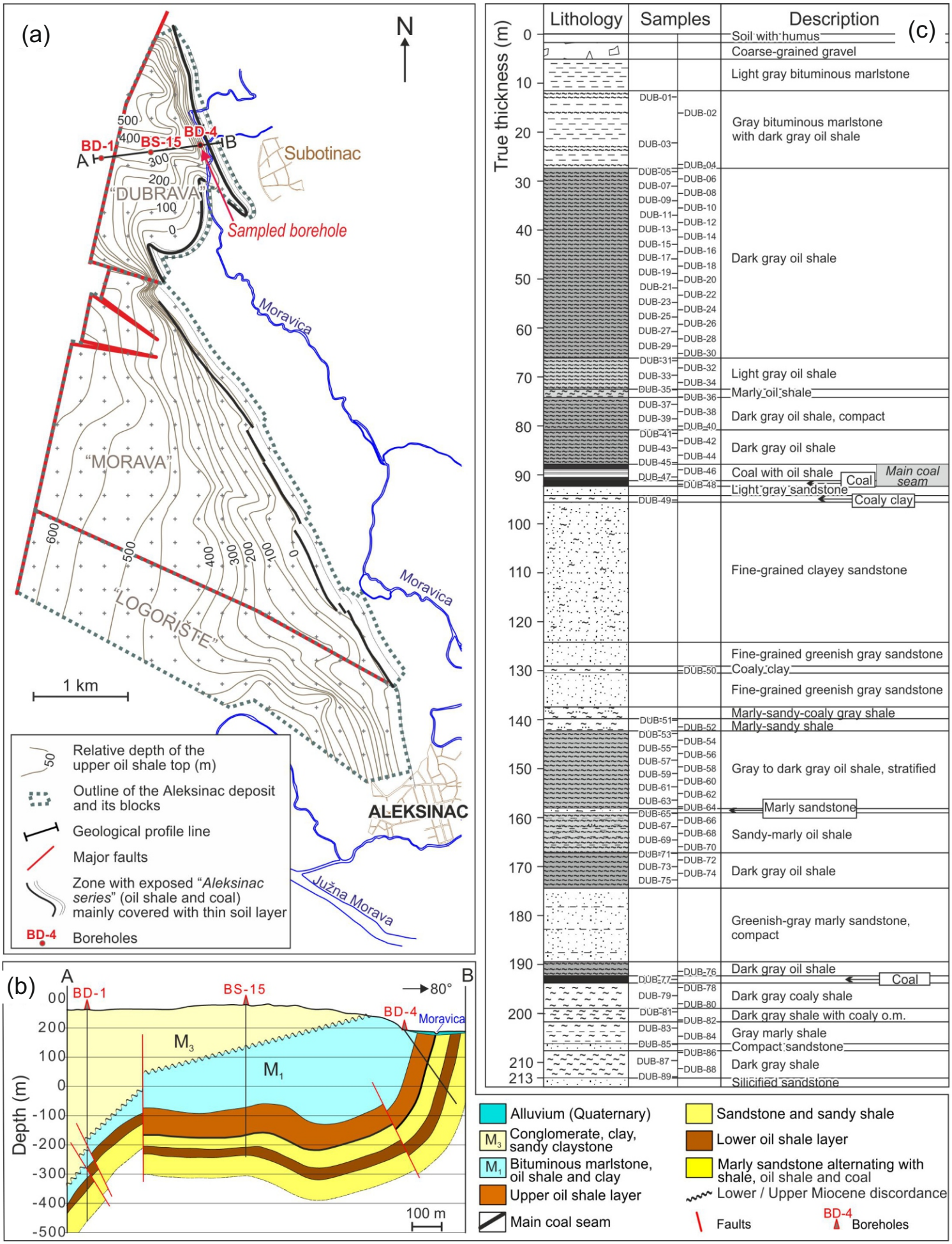

Fig.3:

Figure 04

Fig. 4:

ACCEPTED MANUSCRIPT

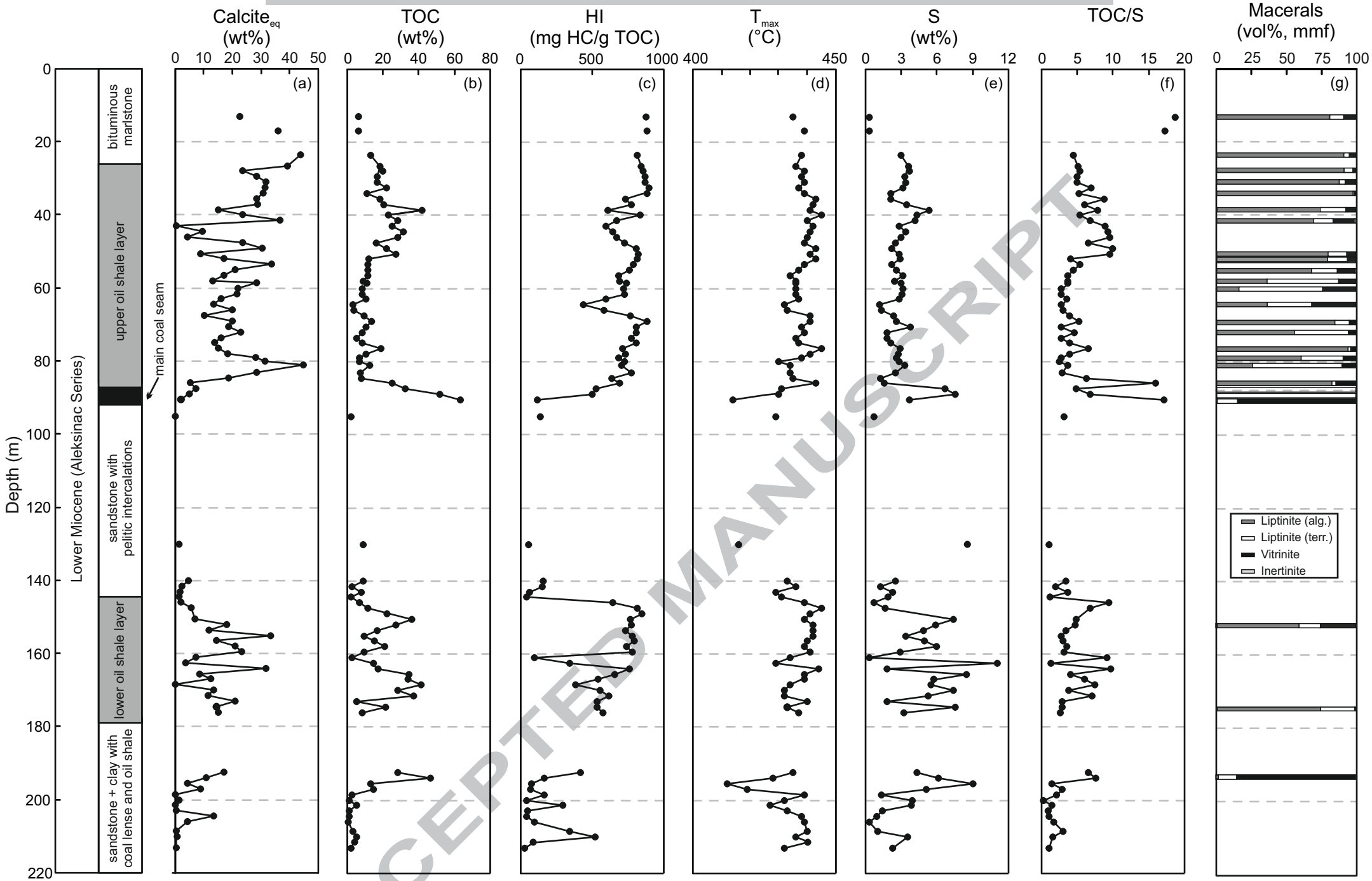

ACCEPTED MANUSCRIPT

Figure 05

ACCEPTED MANUSCRIPT

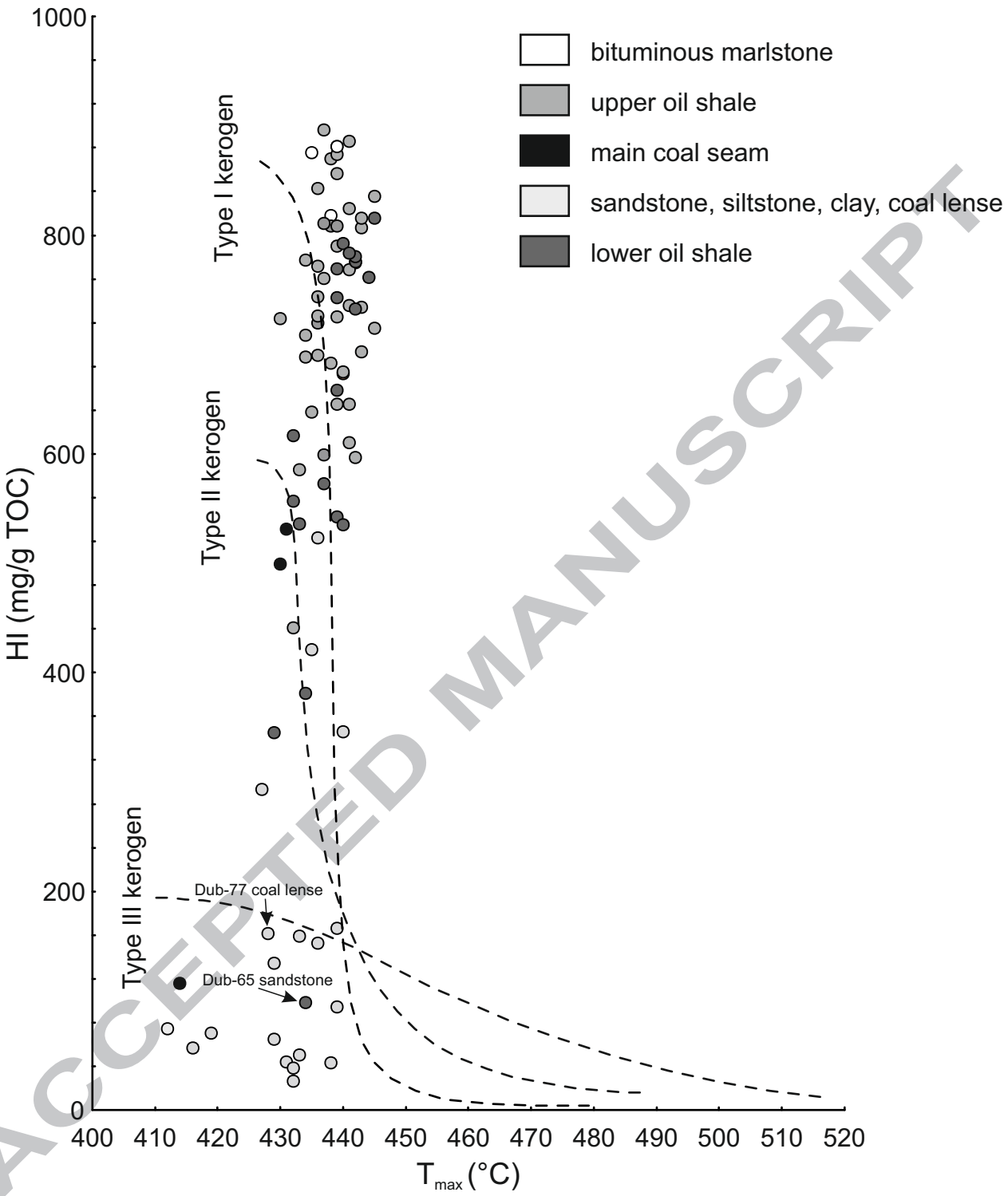

Fig. 5:

ACCEPTED MANUSCRIPT

Figure 06

ACCEPTED MANUSCRIPT

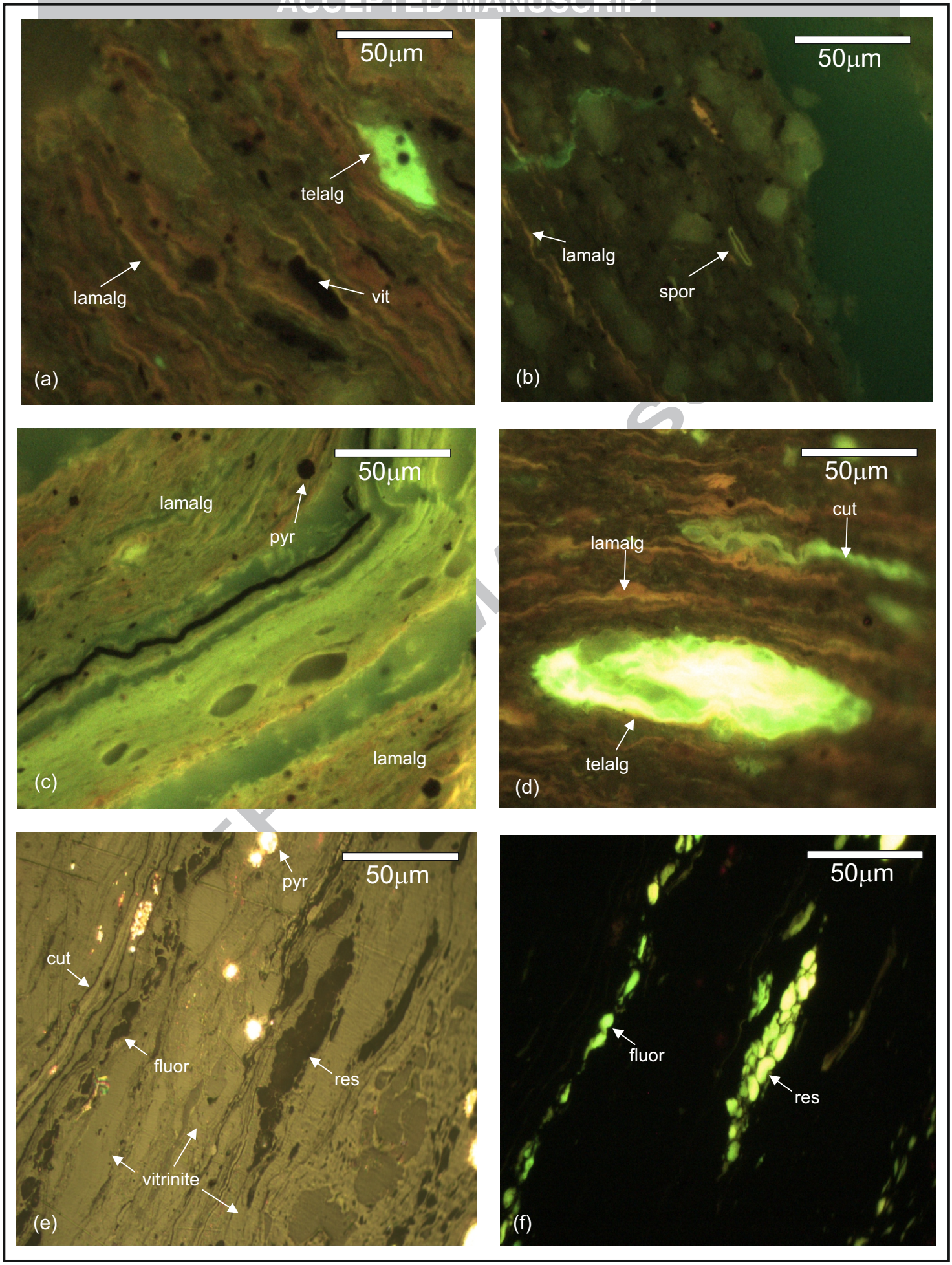

Fig. 6:

Figure 07

ACCEPTED MANUSCRIPT

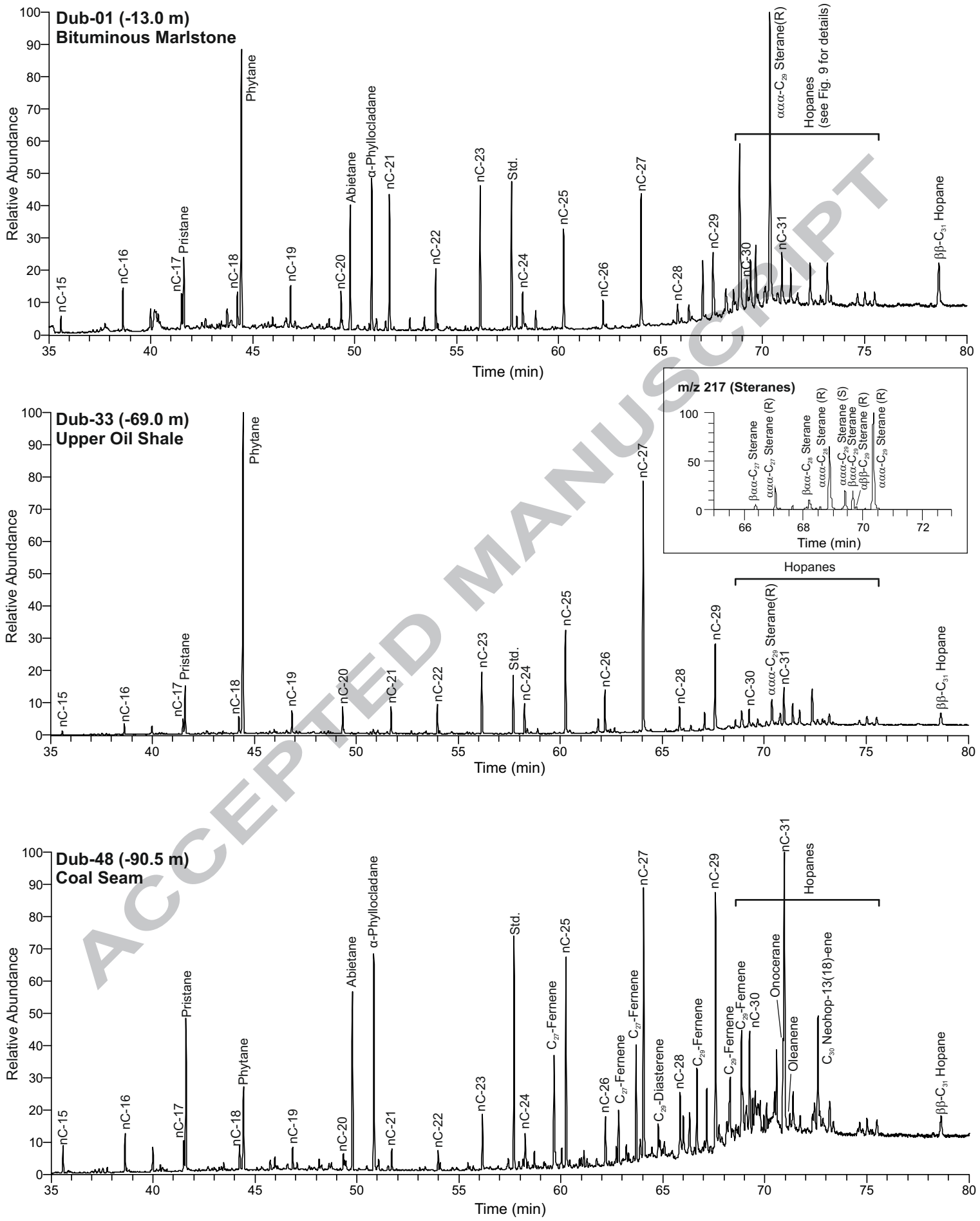

Fig. 7:

Figure 08

ACCEPTED MANUSCRIPT

Fig. 8:

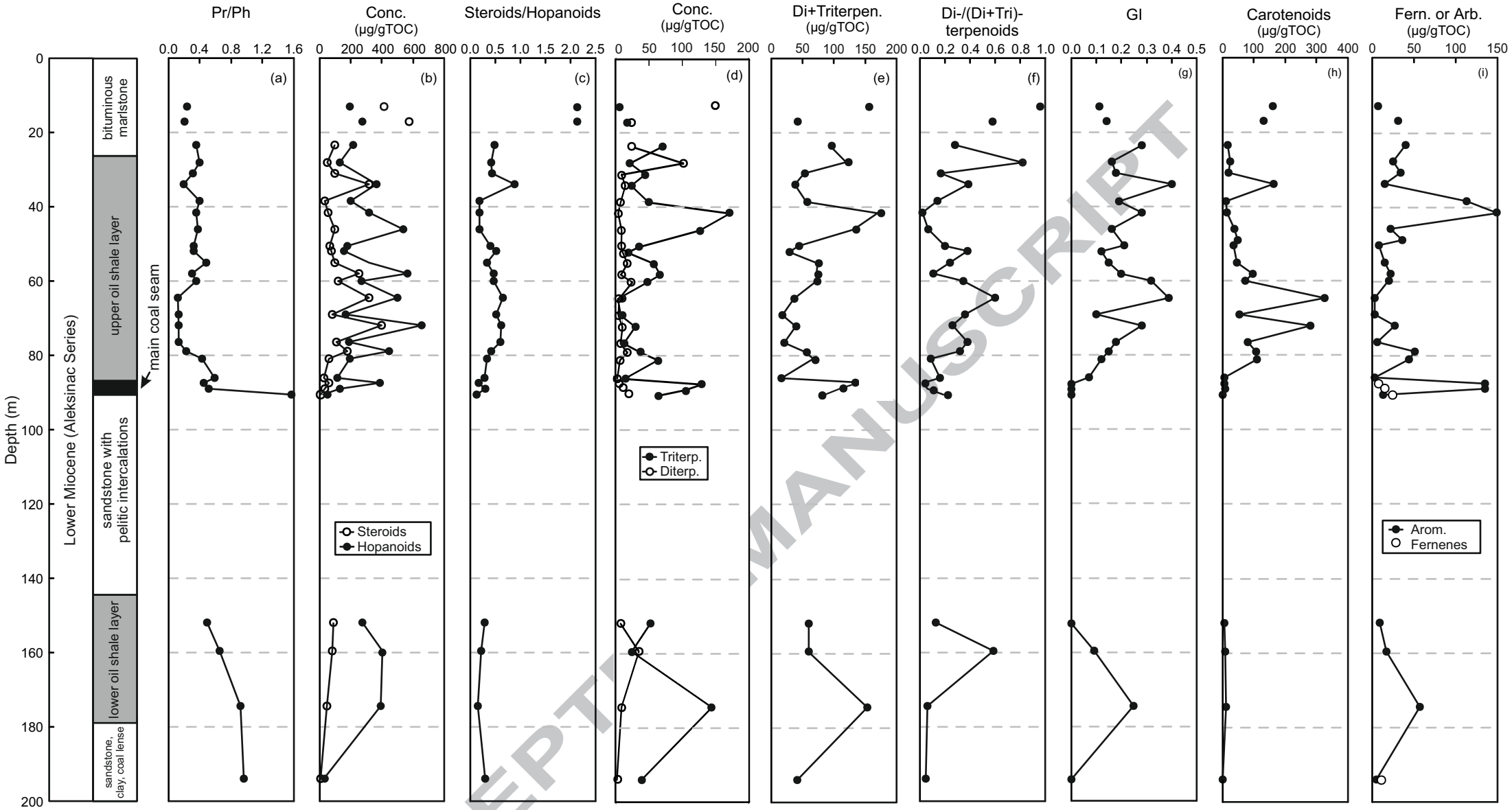

Figure 09

ACCEPTED MANUSCRIPT

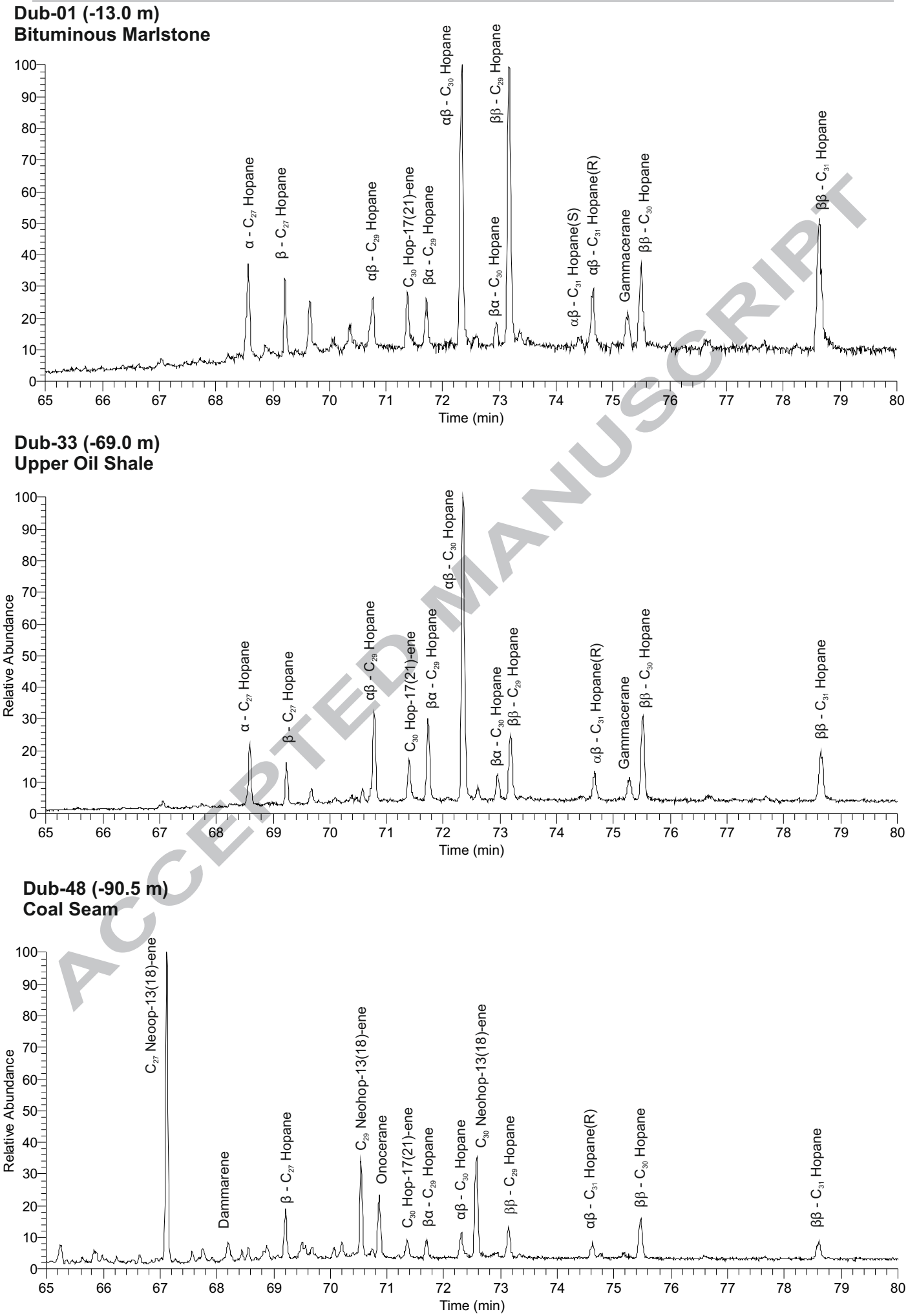

Fig. 9:

Figure 10

ACCEPTED MANUSCRIPT

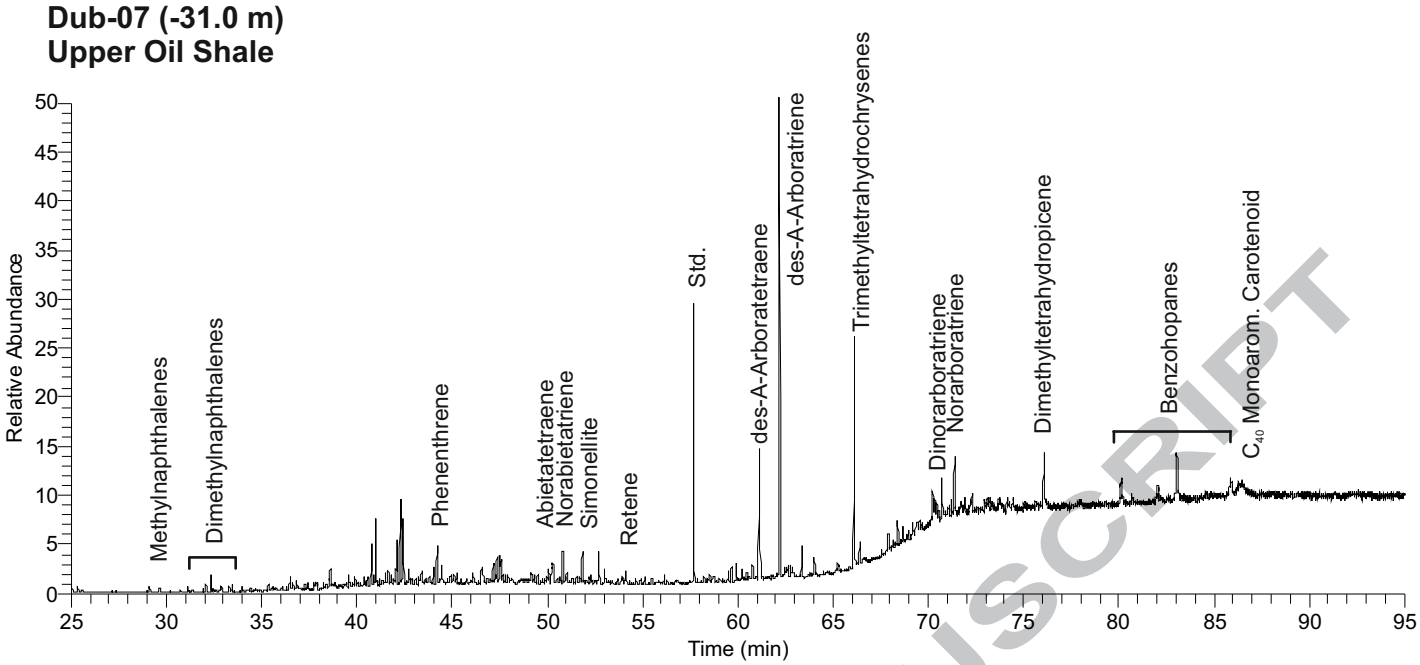

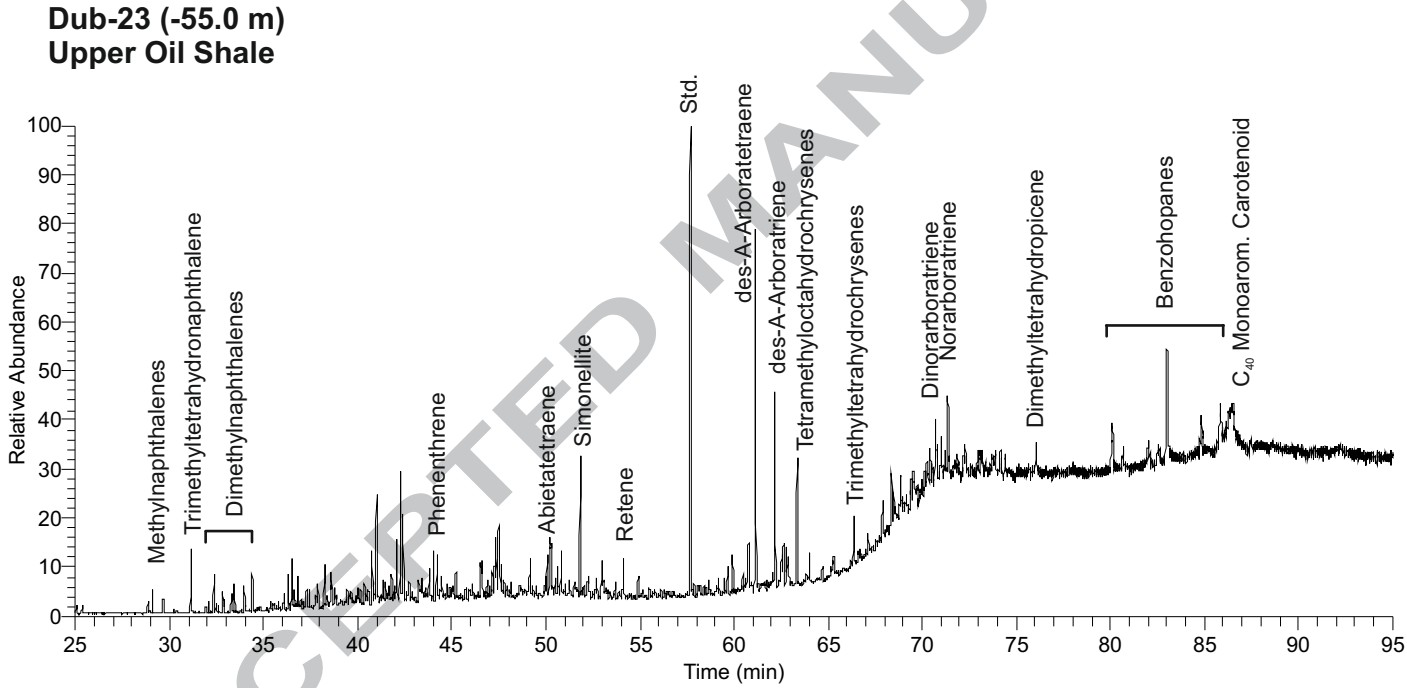

Fig. 10:

ACCEPTED MANUSCRIPT

Figure 11

Fig. 11:

ACCEPTED MANUSCRIPT

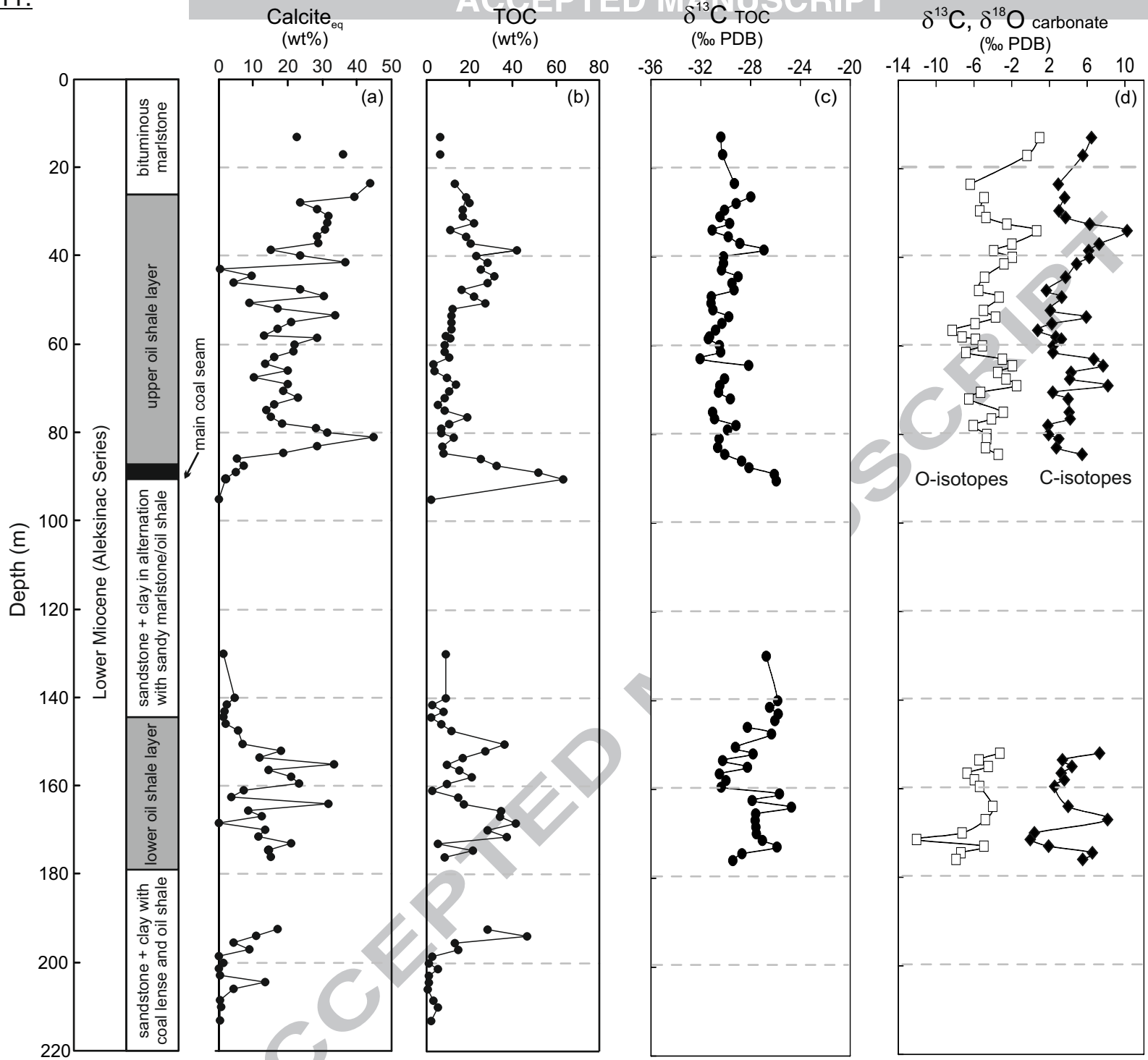

Figure 12

ACCEPTED MANUSCRIPT

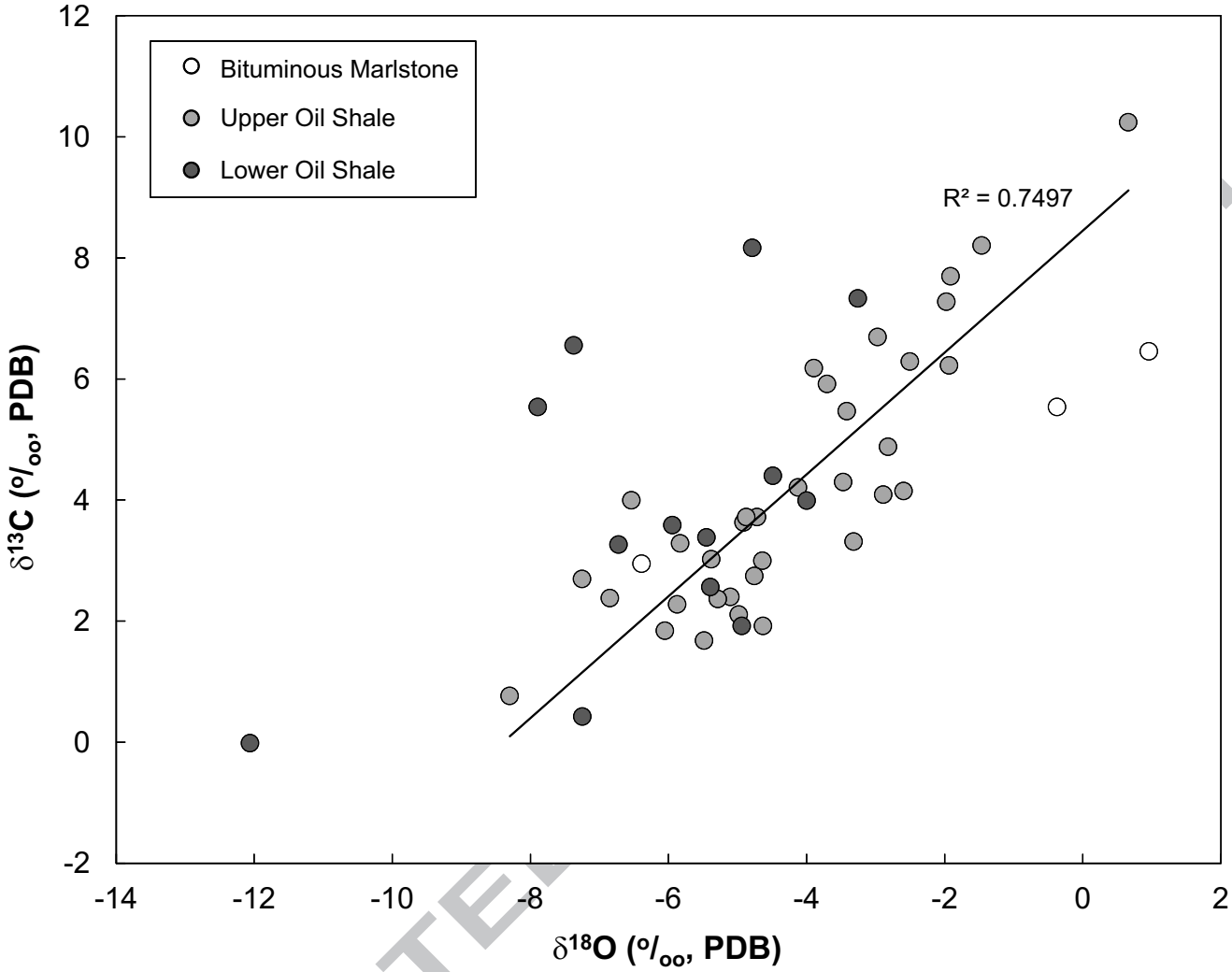

Fig. 12:

ACCEPTED

Figure 13

ACCEPTED MANUSCRIPT

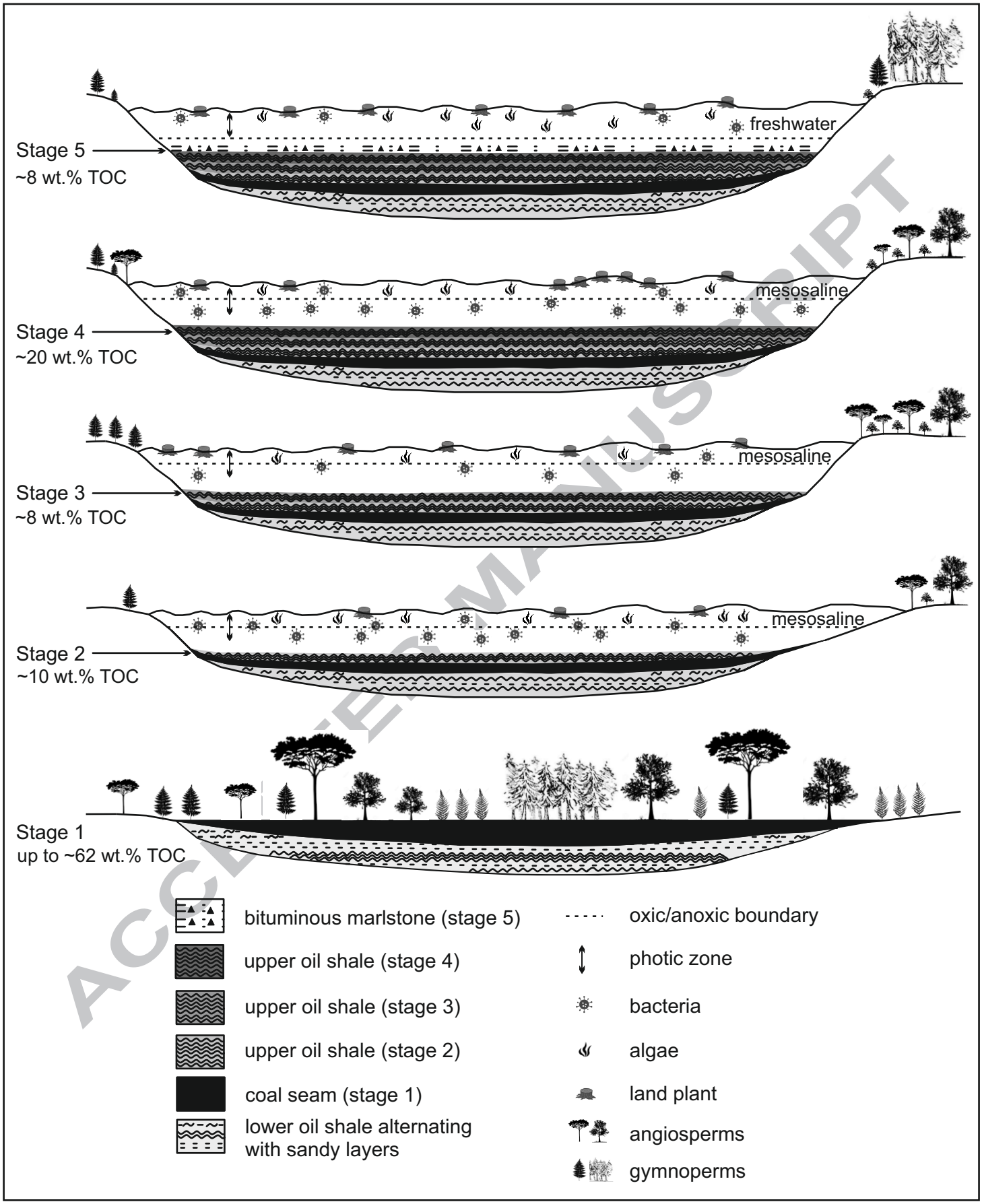

Fig. 13:

Figure 14

ACCEPTED MANUSCRIPT

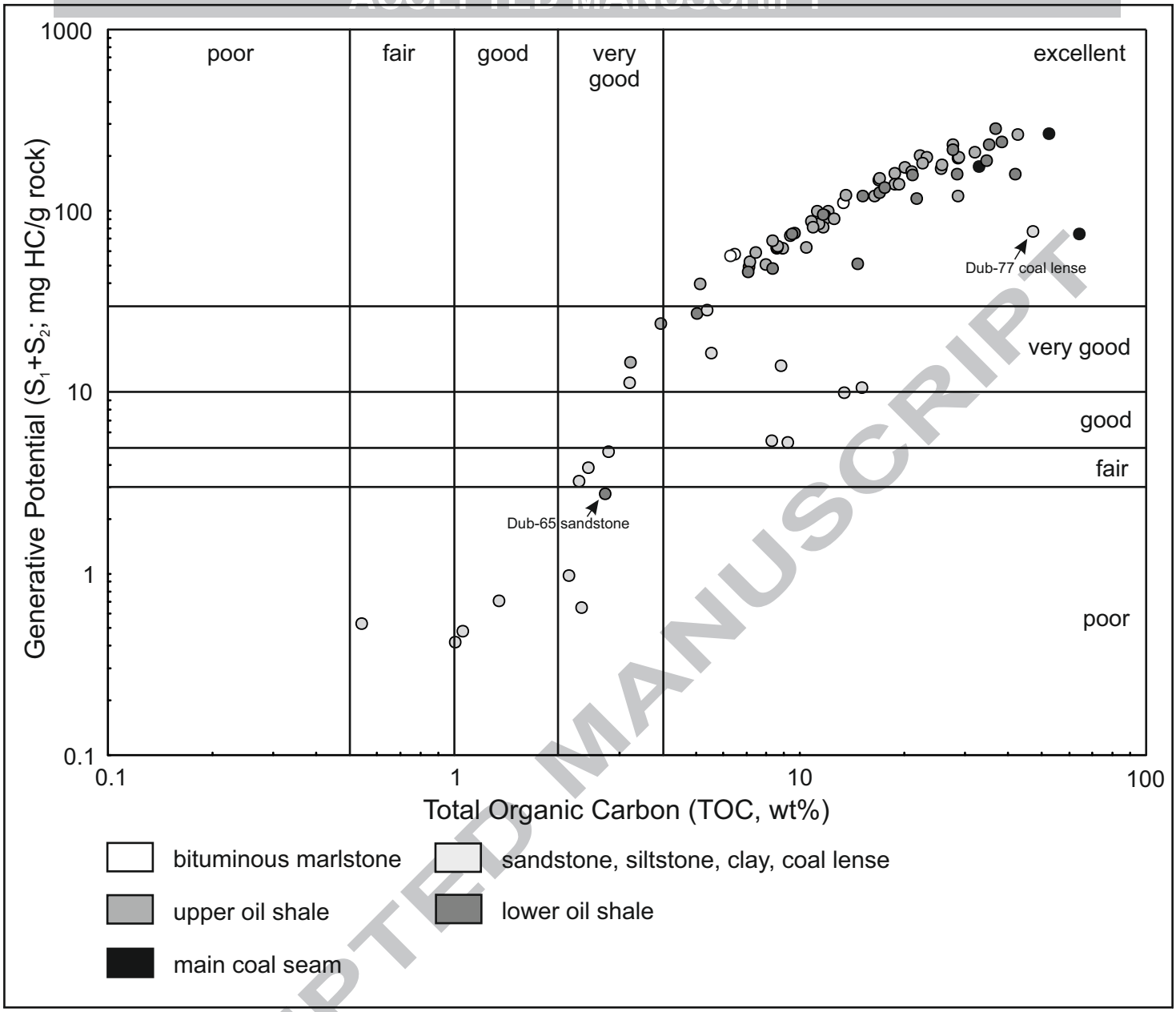

Fig. 14:

ACCEPTED MANUSCRIPT

ACCEPTED MANUSCRIPT

Highlights

- Changes in redox conditions and water colum stratification are outlined
- Carbon cycling in the water column affects $\delta^{13}C$ values of OM
- Immaturity of OM is based on vitrinite reflectance and biomarker ratios
- Excellent source rock quality is indicated by TOC and Rock-Eval data
- Aleksinac oil shale holds a high quality shale oil potential

ACCEPTED MANUSCRIPT